iScience

CellPress
OPEN ACCESS

Article

Transplantation of committed pre-adipocytes from brown adipose tissue improves whole-body glucose homeostasis

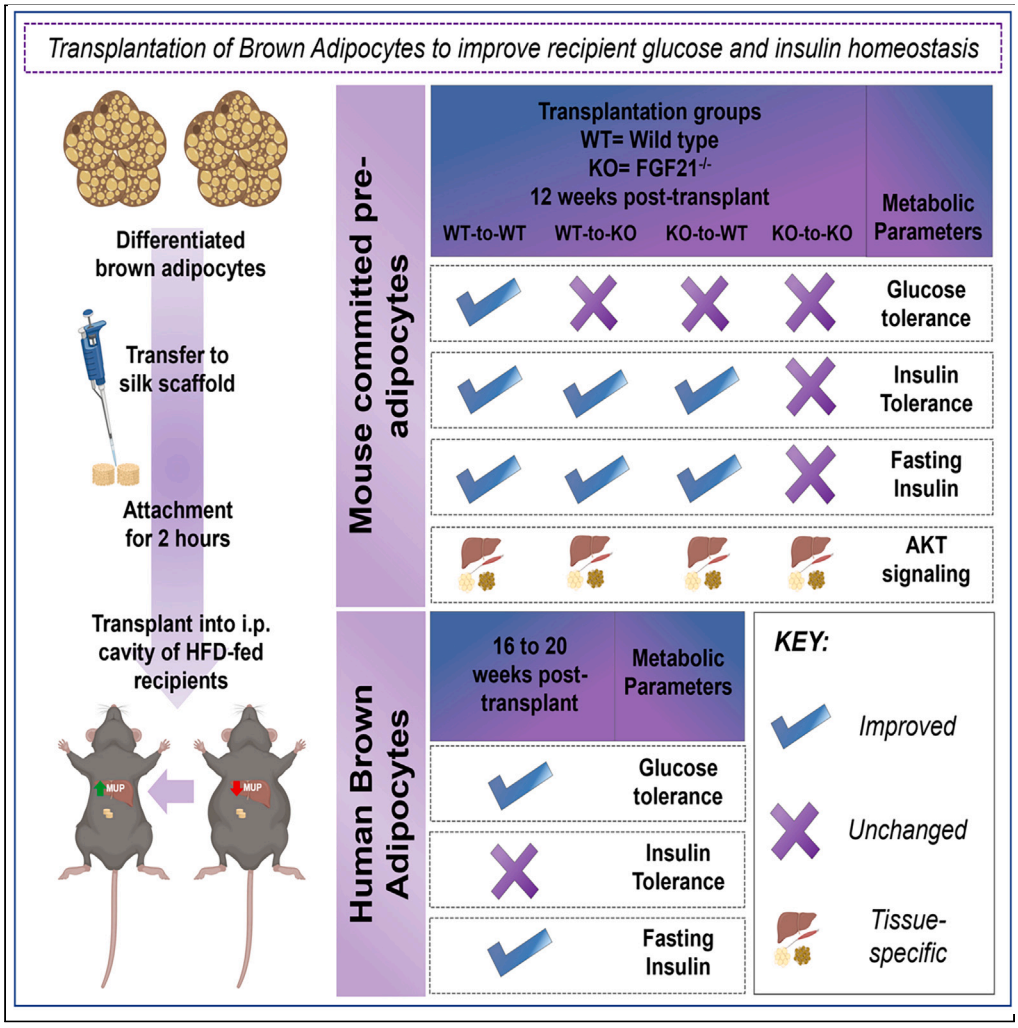

Revati S. Dewal, Felix T. Yang, Lisa A. Baer, ..., Christian Wolfrum, Rosalyn D. Abbott, Kristin I. Stanford

kristin.stanford@osumc.edu

Highlights

Transplantation of differentiated brown adipocytes improves glucose metabolism

2–4 million brown adipocytes improve metabolism after diet-induced obesity in mice

Interactions between FGF21 and AKT mediate metabolism notably via recipient livers

Dewal et al., iScience 27, 108927
February 16, 2024
https://doi.org/10.1016/j.isci.2024.108927

iScience

CellPress
OPEN ACCESS

Article

Transplantation of committed pre-adipocytes from brown adipose tissue improves whole-body glucose homeostasis

Revati S. Dewal,[1] Felix T. Yang,[1,2] Lisa A. Baer,[1,2] Pablo Vidal,[1,2] Diego Hernandez-Saavedra,[1,8] Nickolai P. Seculov,[1] Adhideb Ghosh,[3] Falko Noé,[3] Olivia Togliatti,[1] Lexis Hughes,[1] Megan K. DeBari,[4] Michael D. West,[5] Richard Soroko,[5] Hal Sternberg,[5] Nafees N. Malik,[5] Estella Puchulu-Campanella,[6] Huabao Wang,[6] Pearlly Yan,[6,7] Christian Wolfrum,[3] Rosalyn D. Abbott,[4] and Kristin I. Stanford[1,2,9,*]

SUMMARY

Obesity and its co-morbidities including type 2 diabetes are increasing at epidemic rates in the U.S. and worldwide. Brown adipose tissue (BAT) is a potential therapeutic to combat obesity and type 2 diabetes. Increasing BAT mass by transplantation improves metabolic health in rodents, but its clinical translation remains a challenge. Here, we investigated if transplantation of 2–4 million differentiated brown pre-adipocytes from mouse BAT stromal fraction (SVF) or human pluripotent stem cells (hPSCs) could improve metabolic health. Transplantation of differentiated brown pre-adipocytes, termed "committed pre-adipocytes" from BAT SVF from mice or derived from hPSCs improves glucose homeostasis and insulin sensitivity in recipient mice under conditions of diet-induced obesity, and this improvement is mediated through the collaborative actions of the liver transcriptome, tissue AKT signaling, and FGF21. These data demonstrate that transplantation of a small number of brown adipocytes has significant long-term translational and therapeutic potential to improve glucose metabolism.

INTRODUCTION

Obesity and type 2 diabetes are rapidly increasing in the United States and worldwide.[1] Therapeutic studies to combat obesity and type 2 diabetes have focused on improving glucose metabolism and reducing adiposity. An important tissue to combat the development of obesity and type 2 diabetes is brown adipose tissue (BAT), a thermogenic tissue which can dissipate stored and circulating glucose and lipids in the form of heat.[2,3] The amount and activity of BAT is inversely correlated with obesity in humans, thus increasing BAT mass or activity are important strategies to combat obesity and type 2 diabetes.[2–6] Several studies, including work from our laboratory, have shown that transplantation of whole BAT in rodent models improves glucose metabolism and can mitigate symptoms of type 1 and type 2 diabetes.[2–6]

Similar to transplantation of BAT, increasing the number of active brown adipocytes has the potential to improve metabolic health.[7–10] One recent study utilized CRISPR-Cas9 to transdifferentiate human white pre-adipocytes to UCP1$^+$ brown adipocytes and demonstrated that transplantation of 15–20 million cells reduced obesity and improved glucose tolerance.[10] However, the effect of transplantation of brown adipocytes on metabolic health has not been thoroughly investigated.

BAT is composed of mature adipocytes and the stromal vascular fraction (SVF).[3,11] BAT SVF consists of multiple cell types including pre-adipocytes, mesenchymal stem cells, endothelial cells, and immune cells.[3,11] These pre-adipocytes can be differentiated into mature, functional brown adipocytes. Here, we transplanted pre-adipocytes from murine BAT SVF after differentiation into mature adipocytes (termed "committed pre-adipocytes"), or brown adipocytes from the human AgeX-NP88 line (termed "hBAs") into high-fat fed mice and investigated their effect on glucose metabolism and body composition. Transplantation of only 2 million committed pre-adipocytes from BAT SVF improved whole-body glucose metabolism, fasting insulin, and insulin signaling in multiple tissues 12 weeks post-transplantation. Bulk

[1]Department of Physiology and Cell Biology, College of Medicine, Wexner Medical Center, The Ohio State University, Columbus, OH 43210, USA
[2]Department of Surgery, College of Medicine, Wexner Medical Center, The Ohio State University, Columbus, OH 43210, USA
[3]Laboratory of Translational Nutritional Biology, Institute of Food, Nutrition and Health, ETH Zurich, 8603 Schwerzenbach, Switzerland
[4]Department of Biomedical Engineering, College of Engineering, Carnegie Mellon University, Pittsburgh, PA 15213, USA
[5]AgeX Therapeutics, Inc., 1101 Marina Village Parkway, Suite 201, Alameda, CA 94501, USA
[6]Genomics Shared Resource, Comprehensive Cancer Center, The Ohio State University, Columbus, OH 43210, USA
[7]Division of Hematology, Department of Internal Medicine, The Ohio State University, Columbus, OH 43210, USA
[8]Present address: Department of Kinesiology and Community Health, University of Illinois at Urbana-Champaign, Urbana, Illinois 61801, USA
[9]Lead contact
*Correspondence: kristin.stanford@osumc.edu
https://doi.org/10.1016/j.isci.2024.108927

RNA sequencing revealed a significant effect of the transplanted committed pre-adipocytes on the liver, identifying a potential role for the lipocalin sub-family of major urinary proteins (MUPs) to affect glucose metabolism.

Since previous studies have identified a role of FGF21 to mediate metabolic health, particularly in response to BAT transplantation,[2,12–14] we utilized FGF21$^{-/-}$ mice to determine if FGF21 contributed to the observed metabolic improvements. Transplantation of FGF21$^{-/-}$ committed brown adipocytes in wild-type or FGF21$^{-/-}$ mice, or transplantation of WT committed brown adipocytes into FGF21$^{-/-}$ mice, had a blunted effect on glucose metabolism. In a separate cohort of mice, transplantation of hBAs into high-fat diet (HFD)-fed immunodeficient mice improved glucose homeostasis in recipient mice. Together, these data identify a novel and potentially translatable approach to combat obesity and type 2 diabetes in humans.

RESULTS

Pre-adipocytes from BAT SVF maintain adipogenic capacity and differentiate into mature adipocytes in culture

Cells isolated from murine BAT SVF were cultured and adipogenic differentiation was induced using Adipogenic Induction Media (AIM). Adipocyte-precursor differentiation was observed after 3 days of treatment with AIM as determined by the presence of lipid droplets and increased expression of adipogenic markers (Figures S1A and S1B). These differentiated pre-adipocytes and progenitors, henceforth referred to as "committed pre-adipocytes," were transplanted into recipient mice on day 3 of differentiation.

Committed pre-adipocytes from BAT SVF maintain viability on 3D silk scaffolds, pre- and post-transplantation

To determine viability of cells after transplantation onto silk scaffolds *in vitro*, committed pre-adipocytes from luciferase transgenic mice (Luc^{+}) were incubated on silk scaffolds and injected with luciferin prior to transplantation into mice and bioluminescence was detected using the IVIS (Figure S1C). To determine viability of cell *in vivo*, Luc^{+} committed pre-adipocytes were transferred onto silk scaffolds and then transplanted into the intraperitoneal cavity of wild-type (WT) mice, and the recipients injected with luciferin at 1-week post-transplantation. Bioluminescence was detected using the IVIS *in vivo* imaging (Figure S1D). These data suggest that committed pre-adipocytes maintain viability and luciferase activity *in vitro* and *in vivo* post-transplantation.

Additionally, while cells were present on the scaffolds, luciferase activity was not detected *in vivo* (3 weeks post-transplant) or after extraction of the lipid laden adipocytes from transplanted scaffolds (4 weeks post-transplantation) (Figures S1E–S1H). It is not clear if this was due to infiltration of endogenous adipose tissue causing signal interference, diffusion of transplanted cells from the scaffold, or loss of luciferase activity over time. This is consistent with numerous previous luciferase tracing studies *in vivo* that show that loss of luciferase activity over time does not preclude the functionality of transplanted cells.[15–19] Together, these data show that transplantation of committed pre-adipocytes from BAT SVF using silk scaffolds is an efficient strategy to maintain primary cell function post-transplant.

Transplantation of committed pre-adipocytes from BAT SVF attenuates body weight gain in HFD-fed mice

To determine if transplantation of committed pre-adipocytes from BAT affected body weight or composition, mice were transplanted with empty scaffolds (Sham-WT), whole undifferentiated SVF (1 million cells – SVF 1x; 2 million cells – SVF 2x), or committed pre-adipocytes (1 million cells – interscapular BAT [iBAT] 1x; 2 million cells – iBAT 2x) (Table S2). Body weight gain was attenuated in iBAT 1x and iBAT 2x mice compared to other high-fat fed groups at 12 weeks post-transplantation (Figures 1A and S2A). Additionally, total fat mass was reduced in iBAT 2x mice compared to SVF 2x mice (Figure 1B), and lean mass was increased in SVF 1x, SVF 2x, and iBAT 1x compared to Sham-WT mice 12 weeks post-transplantation (Figure 1C). Lean mass was lower in iBAT 2x mice compared to SVF 1x, SVF 2x, and iBAT 1x, but not Sham-WT, at 12 weeks post-transplantation (Figure 1C). Age matched, untreated chow-fed mice had significantly reduced body weight and fat mass compared to all other groups (Figures 1A and 1B), and reduced lean mass compared to SVF 1x, SVF 2x, and iBAT 1x groups (Figure 1C).

Transplantation of committed pre-adipocytes from BAT SVF improves glucose metabolism and reduces fasting insulin but does not affect thermogenic capacity

Previous studies have established that transplantation of whole BAT improves glucose metabolism in recipient mice.[2–6] To determine if transplantation of committed pre-adipocytes isolated from BAT affects glucose metabolism, we measured glucose tolerance in the previously defined groups. Glucose tolerance was improved in iBAT 2x mice compared to Sham-WT mice at 4-, 8-, and 12-week post-transplantation (Figures 1D, 1E, and S2B). Importantly, glucose tolerance in iBAT 2x mice was improved to the level of age-matched, chow-fed mice at 12 weeks post-transplant (Figures 1D and 1E).

To assess whole-body insulin sensitivity, insulin tolerance tests were performed in all groups at 12 weeks post-transplantation. Insulin tolerance was improved in the iBAT 2x mice to the level of age-matched, chow-fed mice and was significantly lower than all other groups (Figure 1F). Both iBAT 1x and iBAT 2x had reduced fasting plasma insulin compared to Sham-WT, SVF 1x, and SVF 2x mice (Figure 1G), but insulin was significantly increased compared to chow-fed mice. This likely corresponds to the difference in fat mass among chow-fed and iBAT 1x or iBAT 2x mice (Figures 1B and 1G). In summary, glucose tolerance, insulin tolerance, and fasting insulin levels were significantly improved in iBAT 2x mice compared to the Sham-WT group. Glucose and insulin tolerance, but not fasting insulin, were improved in HFD-fed iBAT 2x mice to the level of age-matched, untreated, chow-fed mice. These data demonstrate a powerful role for transplanted committed pre-adipocytes from BAT SVF to improve systemic metabolism in a model of diet-induced obesity.

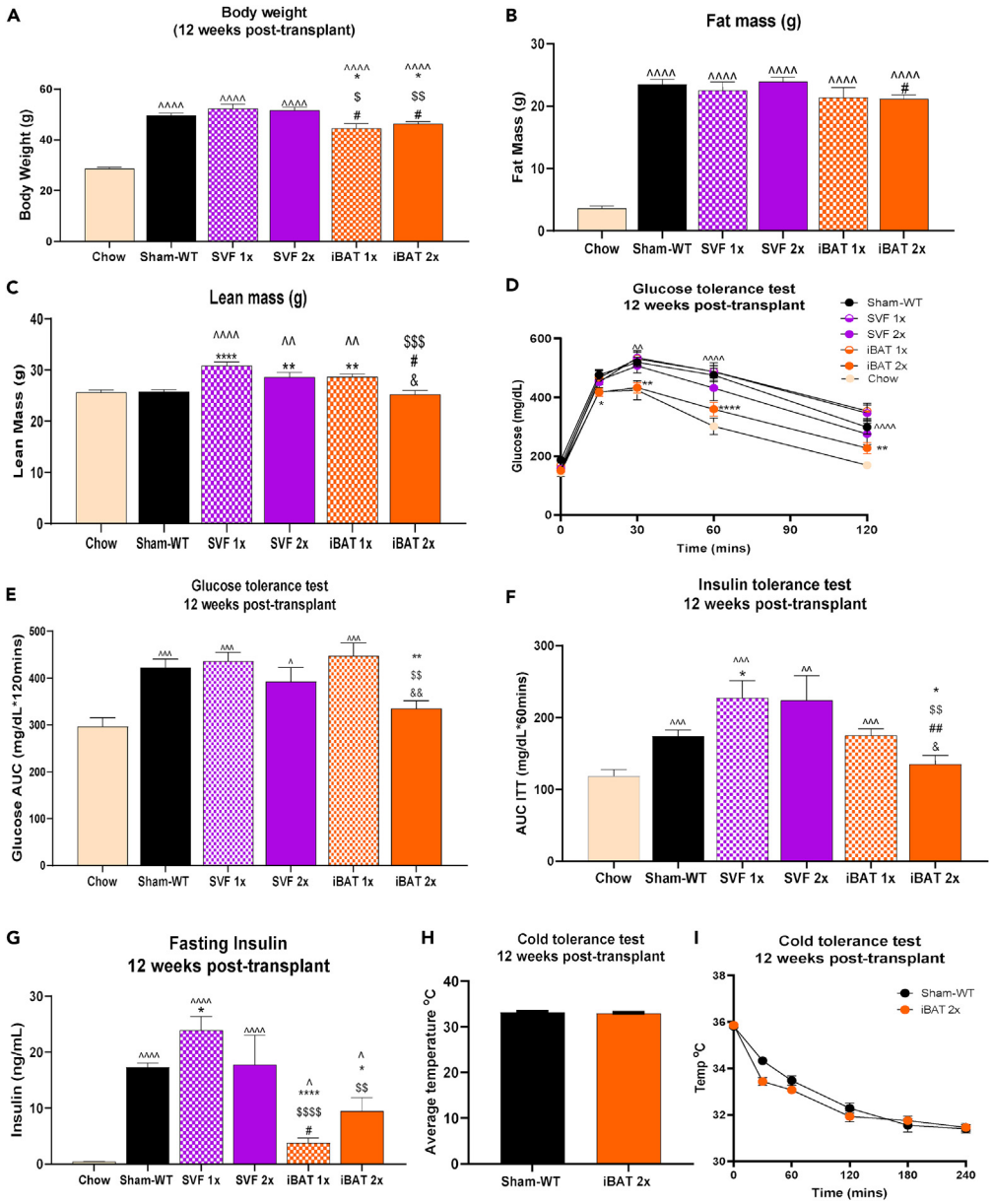

Figure 1. Transplantation of WT committed pre-adipocytes improves whole-body glucose metabolism of WT recipient mice

(A–G) Body weight (A), fat mass (B), lean mass (C), glucose tolerance test (GTT) excursion curve (D), GTT area under curve (AUC) (E), insulin tolerance test (ITT) AUC (F), and plasma insulin levels after 12-h fast (ng/mL) (G), 12 weeks post-transplant (n = 5–46 per group; $^{\wedge}p < 0.05$, $^{\wedge\wedge}p < 0.01$, $^{\wedge\wedge\wedge}p < 0.001$, $^{\wedge\wedge\wedge\wedge}p < 0.0001$ vs. Chow; $^{*}p < 0.05$, $^{**}p < 0.01$, $^{****}p < 0.0001$ vs. Sham-WT; $^{\$}p < 0.05$, $^{\$\$}p < 0.01$, $^{\$\$\$}p < 0.001$, $^{\$\$\$\$}p < 0.0001$ vs. SVF 1x; $^{\#}p < 0.05$, $^{\#\#}p < 0.01$ vs. SVF 2x; $^{\&}p < 0.05$, $^{\&}p < 0.01$ vs. iBAT 1x; two-tailed t-test).

(H and I) Cold tolerance test in WT recipients with average rectal temperature [°C] over 240 min of cold exposure [4°C] (H) and rectal temperature [°C] 0, 30, 60, 120, 180, and 240 min after cold exposure [4°C] (I) (n = 5–7 per group). All data are represented as mean ± SEM.

Since BAT is a thermogenic tissue, we investigated if transplantation of committed pre-adipocytes could mediate thermogenic capacity in the recipient mice. A cold tolerance test was performed in the Sham-WT and iBAT 2x group as those mice had the most pronounced improvements in metabolic health. There was no difference in basal body temperature or after 4 h of cold exposure at 4°C between Sham-WT and iBAT 2x mice (Figures 1H and 1I).

Taken together, these data indicate that transplantation of committed pre-adipocytes from BAT SVF (iBAT 2x) improves glucose and insulin tolerance and reduces fasting insulin. This improvement is specific to transplantation of committed pre-adipocytes as no effects were observed upon transplantation of whole, undifferentiated SVF.

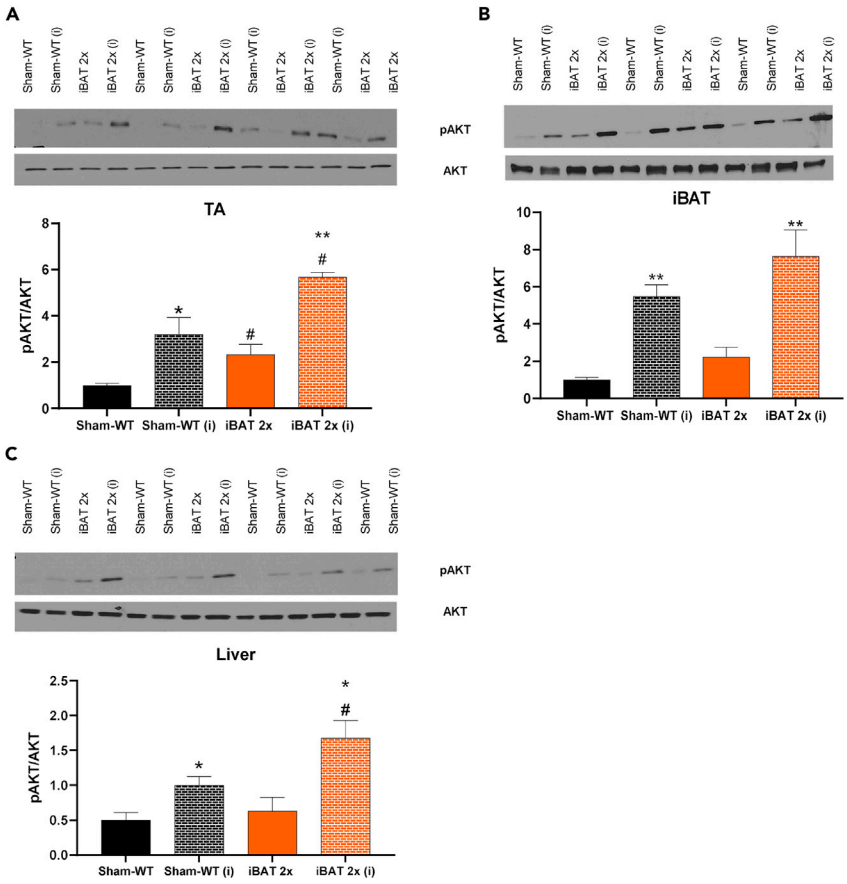

Figure 2. Transplantation of WT committed pre-adipocytes increases pAKT/AKT signaling in tibialis anterior (TA) muscle, iBAT, and liver of WT recipient mice

(A–C) Western blotting protein expression for pAKT/AKT and blots for pAKT and AKT in TA (A), iBAT (B), and liver (C) (n = 3–5 per group; insulin-stimulated conditions depicted using 'i'; *p < 0.05, **p < 0.01 as described [* = insulin effect; # = group effect]; two-tailed t test). All data are represented as mean ± SEM.

Transplantation of committed pre-adipocytes increases AKT phosphorylation in skeletal muscle, adipose tissue, and liver and upregulates expression of metabolic genes in the liver

Transplantation of committed pre-adipocytes from BAT improved glucose tolerance, insulin tolerance, and reduced fasting insulin. To establish which tissues contributed to this improvement in insulin sensitivity, we measured protein expression of pAKT and AKT after acute injection of insulin at 12 weeks post-transplantation, as insulin increases glucose uptake by activation of AKT.[20–22] We also measured expression of genes related to metabolic function and thermogenic activity in iBAT 2x and Sham-WT recipient mice, at 12 weeks post-transplant. As expected, insulin significantly increased the pAKT/AKT ratio in skeletal muscle (TA, tibialis anterior), iBAT, and liver in both Sham-WT and iBAT 2x mice (Figures 2A–2C). This increase in pAKT/AKT was significantly higher in both basal and insulin-stimulated conditions in the TA, and after insulin stimulation in iBAT, liver, and subcutaneous white adipose tissue (scWAT) of iBAT 2x mice (Figures 2A–2C and S2C). There was no difference in pAMPK/AMPK in TA, iBAT, or liver in iBAT 2x mice compared to Sham-WT (Figures S2D–S2F). These data indicate that transplantation of committed brown adipocytes increases the pAKT/AKT ratio in muscle, adipose tissue, and liver, which likely contributes to the improved glucose metabolism and insulin sensitivity in these mice.[20–22]

Expression of genes involved in thermogenesis and glucose metabolism were measured in multiple tissues. There was no activation of thermogenic or metabolic genes in scWAT, perigonadal white adipose tissue (pgWAT), or endogenous BAT, and there was no change in expression of genes involved in glucose metabolism in skeletal muscle (TA). In contrast, genes involved in glucose metabolism were significantly upregulated in the liver of iBAT 2x mice (Figures S3A–S3E). Taken together, these data show that transplantation of WT committed pre-adipocytes to WT recipient mice affects insulin signaling in liver and skeletal muscle, and increases expression of genes involved in glucose metabolism in the liver.

Transplantation of WT committed pre-adipocytes significantly alters expression of pathways associated with glucose, insulin, and lipid metabolism in the liver

Transplantation of 2 million WT committed brown pre-adipocytes significantly upregulated AKT signaling (Figure 2C) and expression of genes related to glucose metabolism (Figure S3B) in the liver of WT recipient mice. Given the contribution of the recipient livers in mediating

metabolic improvements, we investigated changes to the liver transcriptome that could bolster these metabolic improvements via RNA sequencing (RNA-seq) in Sham-WT and iBAT 2x mice. Transcriptomics data showed significant alterations driven by the transplanted adipocytes to modify the liver transcriptome of iBAT 2x mice, as demonstrated via the principal component analysis and differentially expressed genes (Figures 3A, 3B, and S4A). Transplantation of committed pre-adipocytes upregulated signaling in pathways related to glucose, insulin, and lipid metabolism in livers of recipient iBAT 2x mice, concurrent with the observed physiological, protein and gene expression phenotypes in recipient mice (Figures 3C and S4B). In contrast, downregulation of immunological pathways suggests that there are no immunogenic effects of transplanted tissues (Figures 3D and S4C).

In-depth analysis of pathways upregulated in iBAT 2x recipient livers revealed a significant contribution of MUP genes (Figure 3C). MUPs, particularly MUP1, have been implicated in improving glucose metabolism, AKT signaling, and energy expenditure via the liver and skeletal muscle, and are downregulated with diet-induced obesity.[23–26] Transcriptomics data reveal that several genes in the MUP family including MUPs 1, 2, 11, and 12, among others, are significantly upregulated in the liver after transplantation of committed pre-adipocytes (Figures 3B and 3C).

To determine if the RNA-seq data are reflective of functionally relevant changes to MUP expression levels, we measured the gene or protein expression of Mup1, Mup2, Mup11, and Mup12 in the livers of Sham-WT and iBAT 2x mice. Concurrent with the transcriptomics data, gene expression of *Mup1*, *Mup2*, *Mup11*, *and Mup12* (Figure 3E) and protein levels of MUP11 ($p < 0.05$) and MUP12 ($p = 0.056$) were increased (Figures 3F and S5A–S5C) in the liver of iBAT 2x mice. Together, these data demonstrate that the liver transcriptome is significantly altered after transplantation of committed brown adipocytes revealing upregulation of metabolic pathways with no adverse immunological effects. These changes may facilitate the physiological and metabolic improvements observed in iBAT 2x mice, potentially via the MUP lipocalin sub-family.

Transplantation of WT committed pre-adipocytes attenuates body weight gain and improves insulin sensitivity in FGF21$^{-/-}$ recipients

Several studies have determined that FGF21, which can be secreted from BAT or the liver, contributes to improvements in glucose tolerance and insulin sensitivity.[22,27–31] Previous studies have demonstrated that brown adipose tissue can mediate improvements to glucose tolerance and insulin sensitivity through the activity of adiponectin and FGF21,[2,4,13,14,32–38] and several studies have identified a strong correlation of the adiponectin-FGF21 axis and insulin sensitivity.[2,4,13,14,32–38] To determine if adiponectin or FGF21 was responsible for improvements in glucose metabolism after transplantation of committed pre-adipocytes, plasma adiponectin and FGF21 were measured in Sham-WT and iBAT-2x mice. There was no change in adiponectin (Figure S5D), but concentration of FGF21 tended to be increased in iBAT-2x mice 12 weeks post-transplantation (Figure S5E; $p = 0.1$). These data, in conjunction with the observed metabolic improvements, particularly the role of the liver, and previous studies, led us to investigate a role for FGF21 to mediate metabolic improvements after transplantation of 2 million committed pre-adipocytes from BAT SVF.

To determine if the improvements in glucose metabolism and insulin sensitivity after transplantation of committed brown adipocytes were mediated by FGF21, 2 million committed pre-adipocytes isolated from WT donors were transplanted into high-fat fed FGF21$^{-/-}$ recipient mice (WT-to-KO). Body weight and lean mass, but not fat mass, were reduced in WT-to-KO mice compared to Sham-FGF21$^{-/-}$ (Sham-KO) mice (Figures 4A–4C).

FGF21 plays an important role in glucose metabolism and FGF21$^{-/-}$ mice have impaired insulin sensitivity.[22,27–31,39] To determine if transplantation of committed pre-adipocytes from WT mice affected glucose tolerance, glucose tolerance tests were performed in Sham-KO and WT-to-KO mice at 4-, 8-, and 12-week post-transplantation. Similar to previous studies, glucose tolerance was impaired in Sham-KO mice compared to Sham-WT mice 4- and 8-week post-transplant (Figure 4D). WT-to-KO mice had improved glucose tolerance compared to Sham-KO mice 4 weeks post-transplant, but surprisingly, there was no effect on glucose tolerance at 8- and 12-week post-transplantation (Figure 4D).

There was, however, a significant effect of transplantation of committed pre-adipocytes into FGF21$^{-/-}$ mice on both insulin tolerance and fasting insulin. WT-to-KO had improved insulin tolerance and reduced fasting insulin compared to Sham-KO (Figures 4E and 4F). Fasting plasma FGF21 levels were measured 12 weeks post-transplantation and FGF21 was reduced in Sham-KO and WT-to-KO mice compared to Sham-WT mice, but there were no differences between WT-to-KO and Sham-KO mice (Figure 4G). Given the strong improvements to insulin tolerance and insulin sensitivity, it is possible that transplantation of committed pre-adipocytes from BAT SVF mediates metabolic improvements by activating endogenous FGF21 without increasing circulating levels.

Similar to iBAT 2x mice, there was no effect of transplanting committed pre-adipocytes into FGF21$^{-/-}$ mice on thermogenic capacity (Figures 4H and 4I). Taken together, these data suggest that transplantation of WT committed pre-adipocytes into FGF21$^{-/-}$ recipients attenuates body weight gain, improves insulin tolerance, and reduces fasting insulin similar to transplantation into WT recipients, but does not affect glucose tolerance.

Transplantation of WT committed pre-adipocytes attenuates AKT hyperphosphorylation in skeletal muscle and liver of FGF21$^{-/-}$ recipients, and upregulates expression of select metabolic genes in the liver

Previous studies have determined a role for FGF21 to mediate insulin sensitivity and glucose transport through increased AKT phosphorylation.[14,33,35–37] To delineate the mechanism for transplantation of FGF21$^{+/+}$ (WT) committed pre-adipocytes to affect insulin sensitivity in FGF21$^{-/-}$ mice, we measured expression of pAKT and AKT in basal and insulin-stimulated conditions.[20–22] The pAKT/AKT ratio was significantly increased after insulin stimulation in TA and liver of Sham-KO mice. However, this effect was blunted in WT-to-KO mice (Figures 5A–5C, S6A, and S6F). This is consistent with previous studies that have identified a role for insulin stimulation to trigger AKT phosphorylation, independent of FGF21.[12,40] Additionally, and similar to what was observed here, other studies in humans and rats have observed AKT

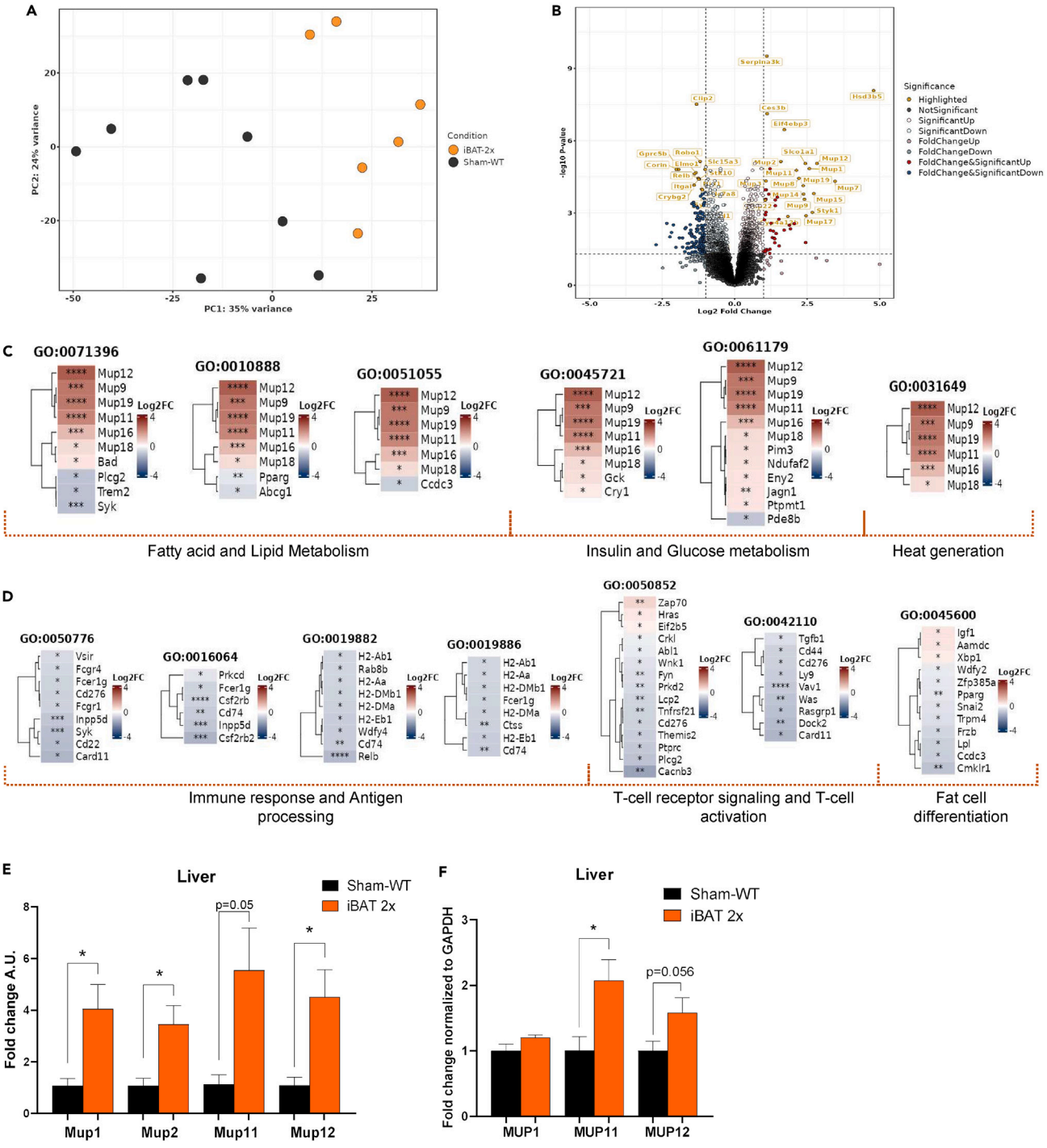

Figure 3. Transplantation of WT committed pre-adipocytes alters pathways associated with glucose, lipid, insulin, and immune processing in the liver of WT recipient mice

(A) Principal component analysis (PCA) plot of Sham-WT and iBAT 2x mice livers (n = 7–9 per group).

(B) Volcano plot depicting differentially expressed genes in iBAT 2x livers versus Sham-WT livers (n = 6–8 per group; significance threshold: 1-fold-change, $p < 0.05$).

(C and D) Tile plots highlighting significantly upregulated (C) or downregulated (D) Gene ontology (GO) biological process (BP) terms and the associated genes based on the over-representation analysis of iBAT 2x livers versus Sham-WT livers (n = 7–9 per group; *$p < 0.05$, **$p < 0.01$, ***$p < 0.001$, ****$p < 0.0001$ vs. Sham-WT).

(E) Gene expression analysis in liver of Sham-WT and iBAT 2x mice, 12 weeks post-transplant (n = 3 per group; *$p < 0.05$ vs. Sham-WT; two-tailed t test).

(F) Western blotting protein expression for MUP1, MUP11, and MUP12 in liver of Sham-WT and iBAT 2x mice, 12 weeks post-transplant (n = 4–6 per group; *$p < 0.05$ vs. Sham-WT; two-tailed t test). All data are represented as mean ± SEM.

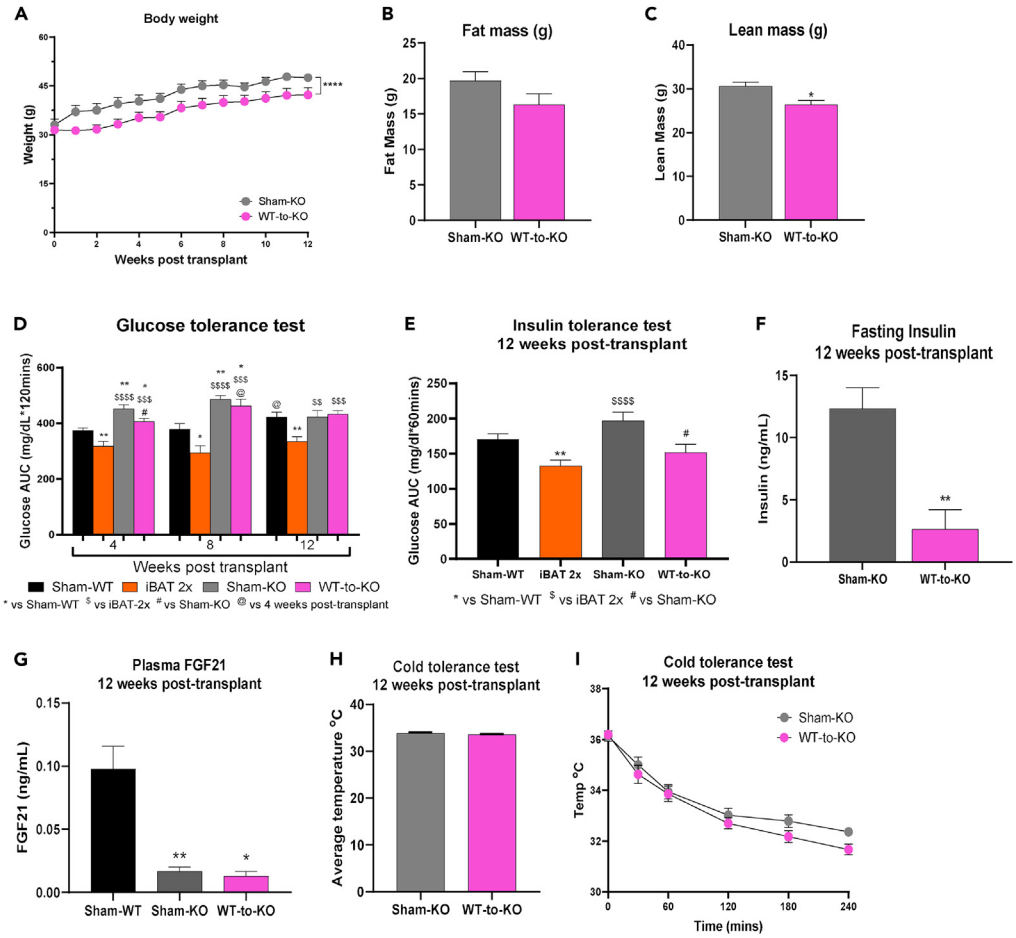

Figure 4. Transplantation of WT committed pre-adipocytes improves metabolic health in FGF21$^{-/-}$ mice

(A–C) Weekly body weight (A), fat mass (B), and lean mass (C), 12 weeks post-transplantation.

(D) GTT AUC data at 4-, 8-, and 12-week post-transplant. (n = 4–31 per group; *p < 0.05. **p < 0.01 vs. Sham-WT; $^{\$\$}$p < 0.01, $^{\$\$\$}$p < 0.001, $^{\$\$\$\$}$p < 0.0001 vs. iBAT-2x; $^{\#}$p < 0.05 vs. Sham-KO; $^{@}$p < 0.05 vs. 4 weeks post-transplant within group; two-tailed t test).

(E) ITT AUC, 12 weeks post-transplant (n = 8–13 per group; **p < 0.01 vs. Sham-WT; $^{\$\$\$\$}$p < 0.0001 vs. iBAT 2x; $^{\#}$p < 0.05 vs. Sham-KO; two-tailed t test).

(F) Plasma insulin levels at 12 weeks post-transplantation after 12-h fast (ng/mL) (n = 3–5 per group; **p < 0.01 vs. Sham-KO; two-tailed t test).

(G) Plasma FGF21 (ng/mL) after 12-h fast, 12 weeks post-transplant (n = 3–12 per group; *p < 0.05, **p < 0.01 vs. Sham-WT; two-tailed t test).

(H and I) Cold tolerance test in FGF21$^{-/-}$ recipients with average rectal temperature [°C] over 240 min of cold exposure [4°C] (H) and rectal temperature [°C] 0, 30, 60, 120, 180, and 240 min after cold exposure [4°C] (I) (n = 4–15 per group). All data are represented as mean ± SEM.

hyperactivation in the heart under conditions of diabetes or cardiovascular disease.[41–43] There were no differences in pAMPK/AMPK among Sham-KO and WT-to-KO mice (Figures S6B–S6E).

These data indicate that transplantation of WT committed brown adipocytes into FGF21$^{-/-}$ mice significantly improves insulin tolerance and reduces fasting insulin, without a corresponding increase in pAKT/AKT. These data suggest that the FGF21-AKT axis may play an obligatory role in mediating glucose tolerance but not insulin sensitivity, indicating a role for FGF21 to mediate insulin sensitivity in the presence (WT recipients) or absence (FGF21$^{-/-}$ recipients) of AKT phosphorylation.

Further investigation of tissue gene expression revealed that, similar to WT recipients, transplantation of committed pre-adipocytes increased expression of select metabolic genes in the liver, including genes from the *Mup* family (Figures 5D and S7A) and did not affect expression of metabolic or thermogenic genes in pgWAT (Figure S7B) of WT-to-KO mice. Similar to iBAT 2x recipients, MUP protein expression was increased in WT-to-KO mice compared to Sham-KO mice (Figures 5E and S7C–S7E).

Transplantation of committed pre-adipocytes from FGF21$^{-/-}$ donors does not affect body composition or glucose tolerance in WT or FGF21$^{-/-}$ recipients, but improves insulin tolerance in WT recipients

Transplantation of WT committed pre-adipocytes improved insulin sensitivity but had different effects on body composition and glucose tolerance in WT and FGF21$^{-/-}$ recipients. To determine if it was the presence of FGF21 in donor adipocytes, and/or endogenous recipient

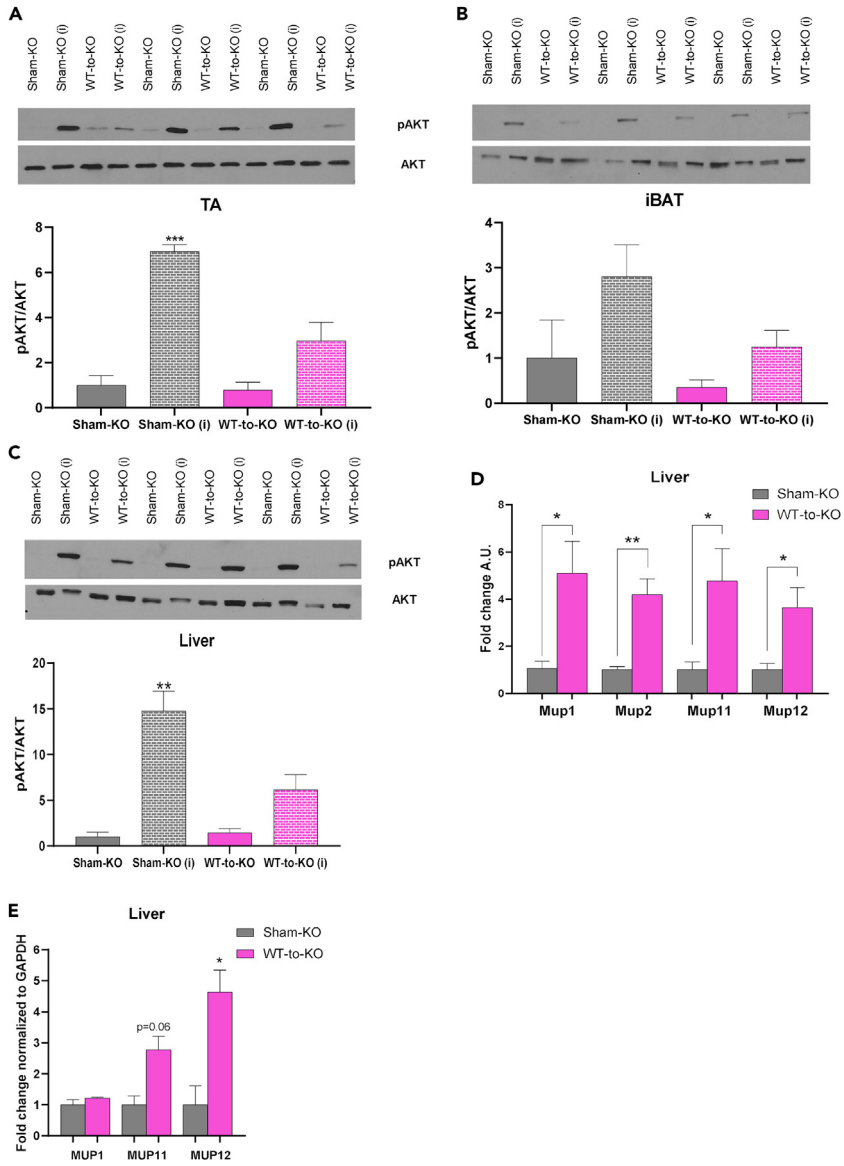

Figure 5. Transplantation of WT committed pre-adipocytes attenuates AKT phosphorylation in skeletal muscle and liver of FGF21$^{-/-}$ recipients

(A–C) Western blotting protein expression for pAKT/AKT and blots for pAKT and AKT in TA (A), iBAT (B), and liver (C) (n = 3 per group; insulin-stimulated conditions depicted using 'i'; *p < 0.05, **p < 0.01 as described [* = insulin effect; # = group effect]; two-tailed t test).

(D) Gene expression analysis in liver of Sham-KO and WT-to-KO mice, 12 weeks post-transplant (n = 3 per group; *p < 0.05, **p < 0.01 vs. Sham-KO; two-tailed t test).

(E) Western blotting protein expression for MUP1, MUP11, and MUP12 in liver of Sham-KO and WT-to-KO mice, 12 weeks post-transplant (n = 4–6 per group; *p < 0.05 vs. Sham-KO; two-tailed t test). All data are represented as mean ± SEM.

tissues that was important for metabolic health, we transplanted committed pre-adipocytes from FGF21$^{-/-}$ mice into WT (KO-to-WT) or FGF21$^{-/-}$ recipients (KO-to-KO) (Table S2). There was no difference in body weight, fat mass, or lean mass among Sham-WT, Sham-KO, KO-to-WT, or KO-to-KO mice at 12 weeks post-transplantation (Figures 6A–6C).

To determine if FGF21 is required to mediate the beneficial effects of transplantation of committed pre-adipocytes on glucose metabolism or insulin sensitivity, glucose tolerance was measured in Sham-WT, KO-to-WT, Sham-KO, and KO-to-KO mice. There was no effect of transplantation of FGF21$^{-/-}$ committed pre-adipocytes on glucose tolerance when transplanted into either WT or FGF21$^{-/-}$ mice (Figures 6D and 6E). These data suggest that transplantation of FGF21$^{+/+}$ cells is important to mediate improvements in glucose tolerance. While KO-to-WT recipients had improved insulin tolerance and fasting insulin compared to all other groups, there was no effect on insulin tolerance or fasting insulin in KO-to-KO mice (Figures 6F and 6G). In fact, Sham-KO and KO-to-KO mice had impaired insulin tolerance

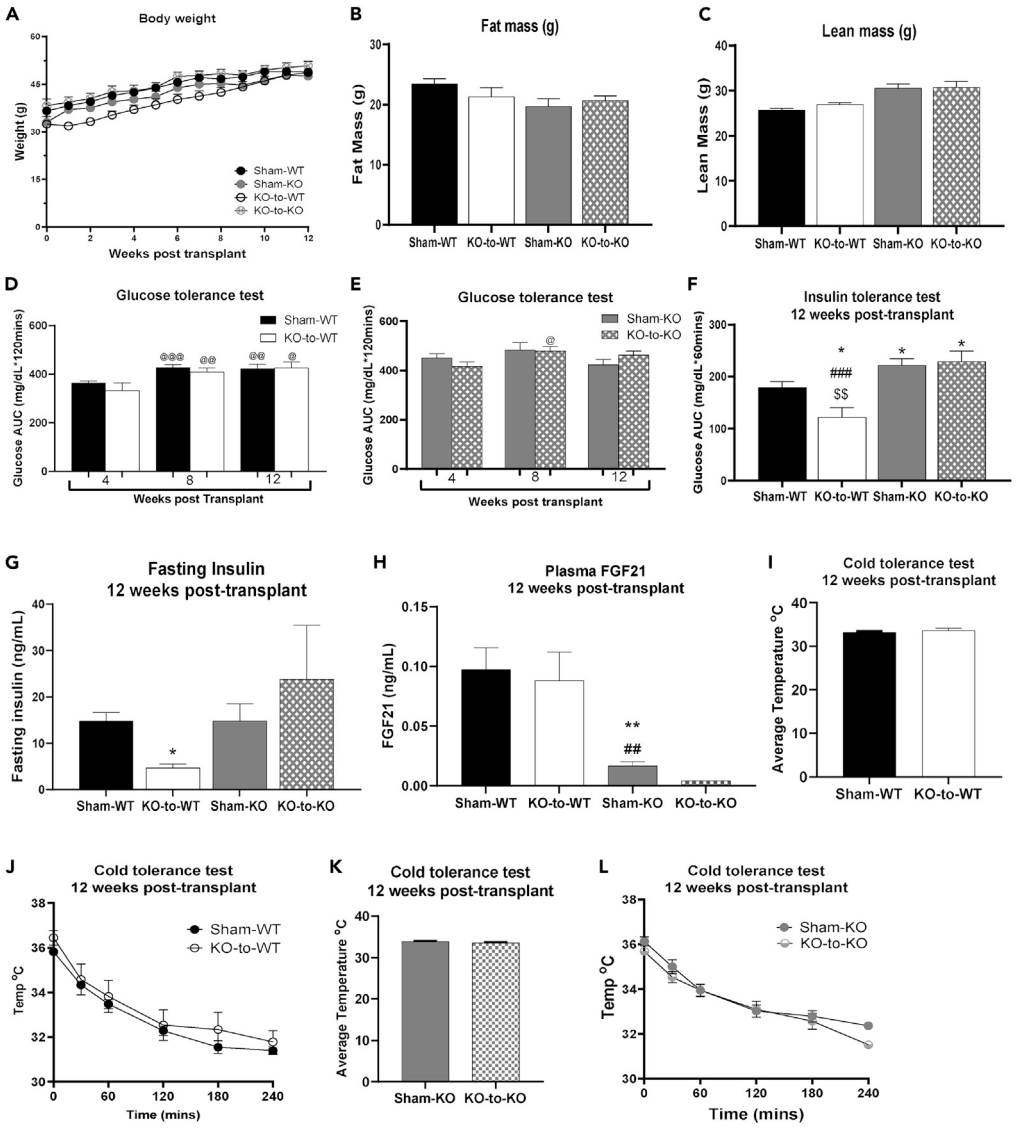

Figure 6. Transplantation of committed pre-adipocytes from BAT SVF of FGF21$^{-/-}$ mice improves insulin tolerance in WT, but not FGF21$^{-/-}$ recipients

(A–C) Weekly body weight (A), fat mass (B), and lean mass (C), 12 weeks post-transplant (n = 5–24 per group).

(D and E) GTT AUC data at 4-, 8-, and 12-week post-transplant (n = 4–46 per group; $^{@}p < 0.05$, $^{@@}p < 0.01$, $^{@@@}p < 0.001$ vs. 4 weeks post-transplant within group; two-tailed t test).

(F) ITT AUC, 12 weeks post-transplant (n = 5–16 per; *p < 0.05 vs. Sham-WT; $^{###}$<p0.001 vs. Sham-KO; $^{\$\$}p < 0.05$ vs. KO-to-KO; two-tailed t test).

(G) Plasma insulin levels at 12 weeks post-transplantation after 12-h fast (ng/mL) (n = 3–14 per group; *p < 0.05 vs. Sham-WT, two-tailed t test).

(H) Plasma FGF21 (ng/mL) after 12-h fast, 12 weeks post-transplant (n = 2–12 per group; *p < 0.05, **p < 0.01 vs. Sham-WT; $^{##}p < 0.01$ vs. KO-to-WT; two-tailed t test).

(I and J) Cold tolerance test in WT recipients with average rectal temperature [°C] over 240 min of cold exposure [4°C] (I) and rectal temperature (°C) 0, 30, 60, 120, 180, and 240 min after cold exposure [4°C] (J) (n = 5–16 per group).

(K and L) Cold tolerance test in FGF21$^{-/-}$ recipients with average rectal temperature [°C] over 240 min of cold exposure [4°C] (K) and rectal temperature [°C] 0, 30, 60, 120, 180, and 240 min after cold exposure [4°C] (L) (n = 6–8 per group). All data are represented as mean ± SEM.

compared to Sham-WT and KO-to-WT mice. There was no difference in fasting plasma FGF21 between KO-to-WT vs. Sham-WT groups, or KO-to-KO vs. Sham-KO groups (Figure 6H), but as expected, Sham-KO and KO-to-KO mice had reduced FGF21 levels compared to Sham-WT and KO-to-WT mice (Figure 6H; KO-to-KO vs. KO-to-WT p = 0.06; KO-to-KO vs. KO-to-WT p = 0.08). Cold tolerance was not different among groups (Figures 6I–6L).

These data indicate that the absence of FGF21 in the recipient mice negates improvements in glucose tolerance, but not insulin tolerance, while lack of FGF21 in both donors and recipients negates all metabolic improvements mediated by transplantation of committed

pre-adipocytes from BAT SVF. This suggests a critical role for recipient FGF21 activity to mediate metabolic improvements after transplantation of committed pre-adipocytes from BAT SVF, without altering circulating levels of FGF21.

Transplantation of FGF21$^{-/-}$ committed pre-adipocytes increases AKT phosphorylation in several endogenous tissues of WT recipients but not FGF21$^{-/-}$ recipients

Transplantation of FGF21$^{+/+}$ (WT) committed pre-adipocytes improved insulin tolerance and reduced fasting insulin when transplanted into WT or FGF21$^{-/-}$ mice. Transplantation into WT mice (iBAT 2x) resulted in increased pAKT/AKT in TA, liver, and BAT (Figures 2A–2C), while WT-to-KO mice did not show increased pAKT/AKT expression compared to Sham-KO mice (Figures 5A–5C). To determine if transplantation of FGF21$^{-/-}$ donor adipocytes mediated pAKT/AKT, endogenous tissues were measured from KO-to-WT and KO-to-KO recipients at 12 weeks post-transplantation under basal and insulin-stimulated conditions. In KO-to-WT mice, where fasting insulin was significantly improved compared to Sham-WT, insulin-stimulated pAKT/AKT was not altered in TA (Figure 7A; $p = 0.07$) or iBAT (Figure 7B) but was increased in liver (Figure 7C) and scWAT (Figure S8A). There was no change in pAMPK/AMPK between Sham-WT and KO-to-WT mice (Figures S8B–S8E).

There was no difference in basal pAKT/AKT signaling among Sham-KO or KO-KO mice, but Sham-KO recipients again showed increased AKT phosphorylation upon insulin stimulation (Figures 7D–7F and S9A).[12] This effect was blunted with transplantation of FGF21$^{-/-}$ committed pre-adipocytes (KO-to-KO mice) (Figures 7D–7F and S9F). There was no change in pAMPK/AMPK between Sham-KO and KO-to-KO mice (Figures S9B–S9E). These data demonstrate that insulin tolerance is improved in WT mice in part by increased pAKT/AKT in the liver and scWAT, even when transplanted with FGF21$^{-/-}$ committed pre-adipocytes. When FGF21 is absent in both donors and recipients, there are no improvements in insulin sensitivity or tolerance.

Overall, these data indicate that FGF21-mediated AKT phosphorylation is correlated with improved insulin sensitivity in WT recipients. In contrast, Sham mice deficient in FGF21 (Sham-KO) show hyperphosphorylation of AKT which does not coincide with improved insulin sensitivity and is attenuated by transplantation of WT or FGF21$^{-/-}$ committed pre-adipocytes.

Transplantation of FGF21$^{-/-}$ committed pre-adipocytes improves expression of metabolic genes in liver of WT recipients but not FGF21$^{-/-}$ recipients

Given the improvements in insulin tolerance and reduced fasting insulin in KO-to-WT recipients but not KO-to-KO recipients, we measured expression of genes related to metabolism and thermogenic capacity in liver and pgWAT of all four groups (Sham-WT, KO-to-WT, Sham-KO, and KO-to-KO). Multiple genes related to glucose metabolism were upregulated in liver of KO-to-WT recipient mice compared to Sham-WT mice (Figure S10A), while select genes (*Hk2*, *Prdm16*) were decreased in pgWAT in KO-to-WT mice (Figure S10B). Expression of *Glut1* and *Glut4* were increased in liver of KO-to-KO recipient mice compared to Sham-KO mice, while there was no change in expression of genes in pgWAT (Figures S10C and S10D). In contrast to iBAT 2x and WT-to-KO recipients, MUP gene or protein expression was not altered in the livers of KO-to-WT or KO-to-KO mice (Figures S10E–S10H and S11A–S11F), suggesting that donor genotype (WT vs. FGF21$^{-/-}$ donors) has a distinctive effect on *Mup* expression in recipient livers. Summarily, these data, alongside the lack of metabolic improvements in KO-to-KO recipients, demonstrate a key role for FGF21 to regulate metabolism after transplantation of committed pre-adipocytes, particularly by modulating gene and protein expression in recipient tissues like the liver.

Transplantation of differentiated hBAs improves glucose tolerance in humanized NSG mice under conditions of diet-induced obesity

Transplantation of 2 million committed pre-adipocytes from BAT SVF improves glucose metabolism in mice with diet-induced obesity. To further determine the translational and therapeutic potential of transplanting a small number of brown adipocytes, cells from a human pluripotent stem cell (PSC) cell line-derived clonal progenitor line designated 'AgeX-NP88' were cultured, differentiated into brown adipocytes (termed ''hBAs''), and transplanted into humanized NSG mice. The hBAs expressed lipid droplets and adipogenic markers including *Ucp1*, *Fabp4*, *and Adipoq* (Figures S12A and S12B). Upon day 3 of differentiation, 2 or 4 million hBAs were transplanted into HFD-fed humanized mice. Transplantation of 2 (HBA 2x) or 4 million (HBA 4x) hBAs did not affect body weight, fat mass, or lean mass of recipient mice when compared to the ''Sham'' (Empty scaffolds) group (Figures 8A–8C). Importantly, after 16 weeks, transplantation of 4 million hBAs (HBA 4x) significantly improved glucose tolerance (Figure 8D) compared to Sham mice. There was no change in insulin tolerance (Figure 8E), but fasting insulin was reduced 20 weeks post-transplantation compared to Sham mice (Figure 8F).

To gain insight into how transplantation affected systemic glucose metabolism, multiple genes involved in glucose metabolism and thermogenesis were measured in endogenous tissues. Genes involved in glucose metabolism were upregulated in liver and scWAT, but not TA, iBAT, or pgWAT of the recipients (Figures S12C–S12H). There was no change in expression of Mup genes in the liver (Figure S12E), or thermogenic genes in endogenous adipose tissues (iBAT, pgWAT, and scWAT) (Figures S12F–S12H).

Taken together, these data suggest that transplantation of human PSC-derived brown adipocytes may have translational potential. In addition, the data suggest that humanized murine models may provide a means of assaying the efficacy of cell transplantation in improving glucose tolerance and metabolic dysfunction under conditions of diet-induced obesity.

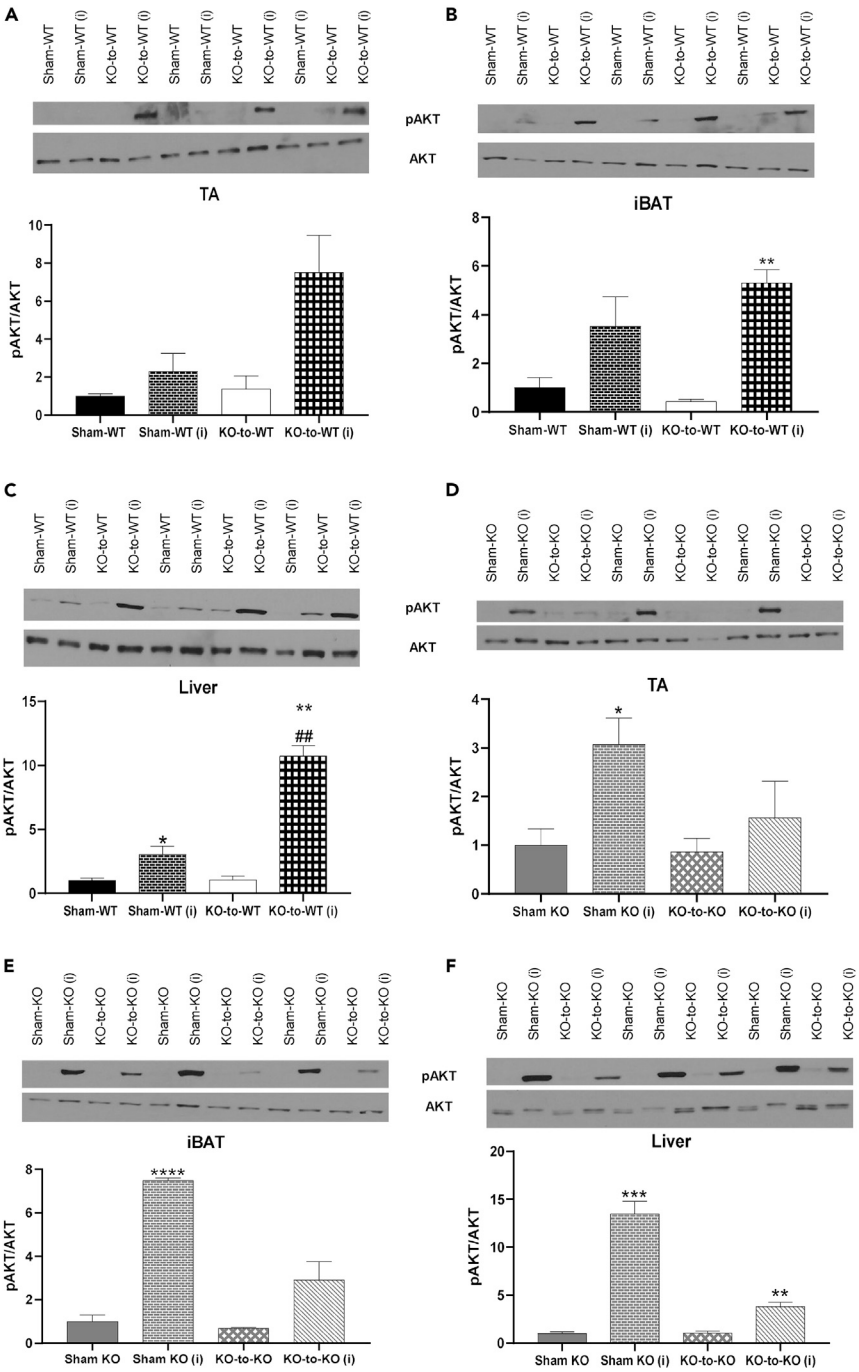

Figure 7. Transplantation of committed pre-adipocytes from FGF21$^{-/-}$ donors increases AKT signaling in TA, iBAT, and liver of WT recipient mice but not FGF21$^{-/-}$ recipient mice

(A–C) Western blotting protein expression for pAKT/AKT and blots for pAKT and AKT in WT recipients in TA (A), iBAT (B), and liver (C).

(D–F) Western blotting protein expression for pAKT/AKT and blots for pAKT and AKT in FGF21$^{-/-}$ recipients in TA (D), iBAT (E), and liver (F) (n = 3 per group; insulin-stimulated conditions depicted using 'i'; *p < 0.05, **p < 0.01 as described [* = insulin effect; # = group effect]; two-tailed t test). All data are represented as mean ± SEM.

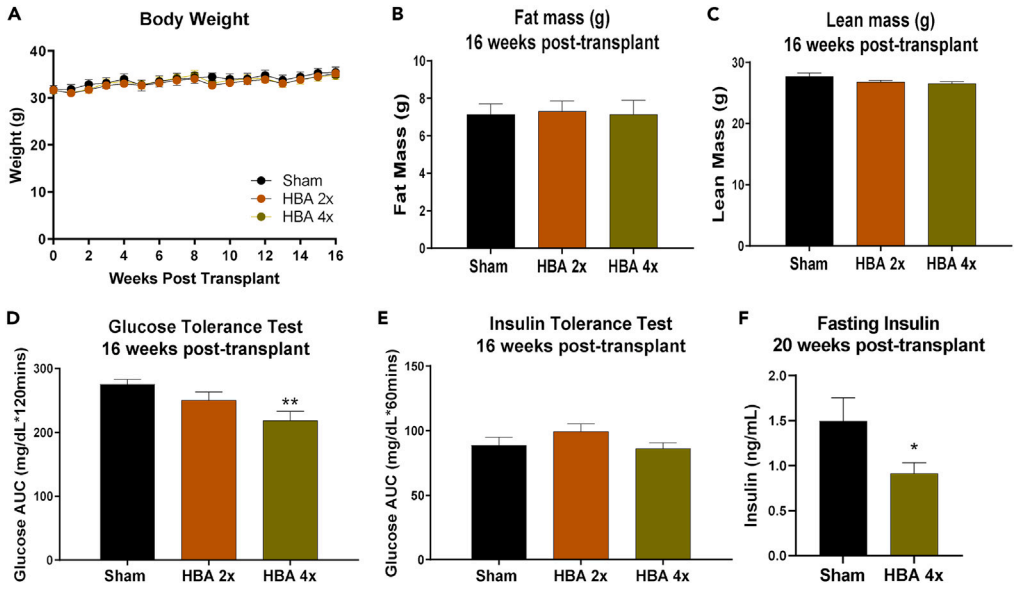

Figure 8. Differentiated human brown adipocytes (hBAs) from AgeX-NP88 cell line improve glucose and insulin tolerance in NSG mice

(A–C) Weekly body weight (A), fat mass (B), and lean mass (C), 16-week post-transplant. (n = 9–10 per group).

(D) GTT AUC data at 16-week post-transplant (n = 9–10 per group; **p < 0.01 vs. Sham 16-week post-transplant; two-tailed t test).

(E) ITT AUC data at 16-week post-transplant (n = 9–10 per group).

(F) Plasma insulin levels at 20 weeks post-transplantation after 12-h fast (ng/mL) (n = 6–9 per group; *p < 0.05 vs. Sham, two-tailed t test). All data are represented as mean ± SEM.

DISCUSSION

Transplantation of BAT is a well-established model to improve glucose metabolism in rodents,[2–6] but the metabolic effects of transplantation of cell types isolated from BAT are relatively understudied.[3,7–10] The data here demonstrate that transplantation of committed pre-adipocytes from BAT SVF improves glucose metabolism and insulin sensitivity in mice and indicate an important role for FGF21.

Previous studies have explored differentiation of stem cells into brown-like adipocytes to counter metabolic impairments.[7–9] A recent study used CRISPR-Cas9 to modify human white adipocytes into UCP1^{+} brown pre-adipocytes. They found that transplantation of 10–20 million of these modified cells improved glucose tolerance and reduced obesity in mice.[10] In the current study, we found that pre-adipocytes isolated from BAT SVF can be cultured, differentiated, and transplanted using inert silk scaffolds. We found that transplantation of 1 or 2 million committed (differentiated) pre-adipocytes reduced fasting insulin, and transplantation of 2 million committed pre-adipocytes improved glucose metabolism and increased insulin sensitivity 12 weeks post-transplantation. This suggests a potential dose-dependent effect of transplanting committed pre-adipocytes. A study that transplanted a different category of scaffolds (Poly(lactide-co-glycolide); PLG based) into epididymal fat pads of HFD-fed mice found similar improvements in fasting insulin without corresponding changes in glucose tolerance. It is possible that 1 million committed pre-adipocytes or PLG particles act as stimuli to trigger limited metabolic improvements but not a widespread metabolic overhaul.[44]

Determining cell viability post-transplantation is an important validation step prior to metabolic analysis. Previous transplantation studies have used fluorescent (GFP), bioluminescent (luciferase), or enzymatic (Beta-galactosidase) transgenes to determine cell viability.[7,15–19,45–53] Using these strategies, most studies showed that viable cells were detectable 1–2 weeks post-transplant with only a few detecting cells more than 3–4 weeks post-transplantation.[7,15–19,45–53] Most of the previous studies carried out subcutaneous transplants and with whole tissue or 5–30 million cells.[7,15–19,45–53] Our data are consistent with these previous transplantation models despite performing intraperitoneal transplantation and with a lower cell number. Interestingly, most studies were unable to detect transplanted cells more than 4 weeks post-transplantation, and studies that used luciferase activity for cell detection found that luciferase activity was not detected more than 1–2 weeks post-transplant by either bioluminescence or gene expression.[15–19,45] One study that transplanted luciferase-positive islet cells subcutaneously in rats showed that luciferase activity dropped over 50% in two weeks[18] but the improvements in glucose homeostasis were detected continuously up to 6 weeks post-transplant.[18] These studies are consistent with our data indicating that lack of luciferase activity does not undermine viability of cells or preclude their ability to induce metabolic improvements post-transplant. It is possible that in our study, infiltration of endogenous adipose tissue onto the scaffolds obfuscates the luciferase signal, or the transplanted cells diffuse out of the scaffolds or lose luciferase activity over time. Importantly, while luciferase activity was only detectable *in vivo* early on, the metabolic benefits prevailed long term, up to 12 weeks post-transplant, stimulating endogenous tissues including the liver and TA to improve systemic metabolism.

As FGF21 is an important mediator of glucose metabolism, insulin sensitivity, and obesity, we investigated the role of FGF21 to contribute to the improved glucose and insulin tolerance and reduced fasting insulin observed with transplantation of committed brown

adipocytes.[2,13,22,27–31,34,39,40,54–56] By transplanting cells with or without FGF21 into either WT or FGF21$^{-/-}$ mice, we establish that FGF21 affects glucose tolerance, insulin tolerance, and insulin sensitivity. When FGF21 is produced by both donor cells and recipients, glucose and insulin tolerance are improved and fasting insulin is reduced; when FGF21 is produced in either donor cells or recipients, improvements are seen only in insulin tolerance and reduced fasting insulin, while the complete absence of FGF21 negates all metabolic improvements. These data identify an essential role for cells producing FGF21 to regulate and improve metabolic health. Interestingly, while we observe a tendency for FGF21 to be elevated in iBAT 2x mice, most metabolic alterations with transplantation occur without changes to absolute concentrations of circulating FGF21 in other recipient mice. This suggests activation of existent FGF21 to affect metabolism via endogenous tissues rather than increased concentration in circulation. These data corroborate another study which showed that UCP1+ adipocytes do not increase circulating FGF21 levels but can impact energy expenditure in conjunction with FGF21 activity.[57] This is important because while the use of FGF21 agonists or injections is technically easier to administer, previous studies attempting it reported little success, also in part due to its short half-life, thus making chronic FGF21 activity difficult to achieve.[32,38,58–61] As a result, inducing cell-based FGF21 expression or activation of existing, endogenous FGF21 could be a more sustainable approach to promote its metabolic benefits.

An important finding of this study was a role for transplanted brown adipocytes to mediate insulin sensitivity. When FGF21 was present, insulin sensitivity was improved. In contrast, when FGF21 was absent in both donors and recipients, there was no improvement in insulin sensitivity. Given that insulin can stimulate AKT signaling to increase glucose uptake into tissues, and FGF21 and AKT have a strong interactive relationship, we measured activation of pAKT in our transplantation models.[12,13,22,34,40,54–56] We found that transplantation of FGF21$^{+/+}$ (WT) or FGF21$^{-/-}$ committed pre-adipocytes increased AKT phosphorylation in endogenous tissues of WT recipients but not FGF21$^{-/-}$ recipients. However, insulin sensitivity was improved with transplantation of FGF21$^{+/+}$ (WT) cells into both WT and FGF21$^{-/-}$ recipients, as well as transplantation of FGF21$^{-/-}$ cells into WT recipients. These data indicate that transplantation of committed pre-adipocytes mediates insulin sensitivity through increased AKT signaling only in WT recipients. When WT committed pre-adipocytes are transplanted into FGF21$^{-/-}$ mice, insulin sensitivity is improved independent of an increase in AKT phosphorylation. Contrarily, AKT was hyperphosphorylated in Sham-KO (FGF21$^{-/-}$) mice, consistent with previous studies showing AKT hyperphosphorylation in FGF21$^{-/-}$ mice, and in humans or rat models of diabetes or cardiovascular disease.[12,13,22,34,40–43,54–56] While a specific cause for AKT hyperphosphorylation is not known, a previous study identified independent and additive actions of insulin and FGF21 to increase pAKT/AKT in human adipocytes derived from adipose tissue stem cells,[12] and another showed increased pAKT/AKT in visceral WAT of FGF21$^{-/-}$ mice.[40] It is possible that this may occur due to non-canonical insulin signaling, adiponectin-mediated or compensatory activation in the absence of FGF21. Understanding the root cause for hyperactivation of AKT will require further investigation and is outside the scope of this study. In this study, hyperphosphorylation of AKT did not coincide with metabolic improvements and was attenuated by transplantation of FGF21$^{+/+}$ (WT) or FGF21$^{-/-}$ committed pre-adipocytes. These data suggest that FGF21 could affect insulin sensitivity through alternative mechanisms in FGF21$^{-/-}$ mice and warrants further investigation.

Furthermore, this study looked at changes to tissues involved in glucose uptake like TA, iBAT, liver, scWAT, and pgWAT. In WT and FGF21$^{-/-}$ recipient mice with improved glucose metabolism, genes involved in glucose metabolism were upregulated only in the liver, while AKT signaling was improved in the liver, TA, and scWAT. Given the particularly strong changes in protein and gene expression in livers of WT recipient mice, we performed RNA sequencing to illuminate tissue-specific transcriptomic changes. Pathways pertaining to glucose and fatty acid catabolism were upregulated while pathways governing immune responses, phagocytosis, and others were downregulated in iBAT 2x livers compared to Sham-WT livers. Not only are these data concurrent with the observed metabolic improvements in iBAT 2x mice, but they also highlight that no negative immunogenic implications of transplanted committed pre-adipocytes are seen in the neighboring liver tissue, 12 weeks after transplantation.

Analysis of differentially expressed genes in iBAT 2x livers identified a lipocalin family sub-group, called MUPs, that were significantly upregulated in iBAT 2x mice compared to Sham-WT mice. MUPs, considered to be largely homogeneous in their sequences and functions, are produced predominantly in the liver, in a sexually dimorphic manner, skewed toward male mice.[23–26] MUPs have been implicated in some studies to have a role in glucose metabolism, insulin sensitivity via AKT signaling, and energy expenditure, by affecting the liver and skeletal muscle.[23–26] Interestingly, the expression of MUPs is decreased with diet-induced obesity.[23–26] Here, we found that MUPs were significantly increased in recipient livers. Given their role in mediating AKT signaling[23] and metabolic pathways,[23–26] these data present the possibility that MUPs might affect insulin signaling in an FGF21-dependent or independent manner.

While the role of MUPs in type 2 diabetes and diet-induced obesity is not well defined, works including this study pave the way for further research in understanding their function and metabolic implications.[23–26] To that end, it is an important constraint to note that MUPs have no analogs in humans.[26] This means that similar pathways in humans are likely governed by alternative proteins which will require further study.[26] Additionally, while MUPs and their effects on metabolism are present in both male and female mice, these effects are stronger in male mice.[26] Thus, it will be vital to determine how MUP-based signaling functions in female mice. In totality, these data reiterate the fact that physiological function is rarely governed by a single signaling pathway but rather by complex interactions, in this case between FGF21, AKT-based insulin signaling, the MUP family, and possibly others.

Additional studies are needed to focus on alternative signaling proteins that interact with FGF21 and the role of additional endogenous tissues like the heart, gut, and other skeletal muscles on glucose tolerance and insulin sensitivity in both FGF21$^{+/+}$ (WT) and FGF21$^{-/-}$ recipients.[62] Additionally, while recent studies have identified an endocrine and paracrine role for both BAT and FGF21,[22,34,63] several other FGFs including FGF1, FGF6, FGF9, and FGF15/FGF19 have been previously implicated in affecting whole-body glucose homeostasis and obesity.[27,29,31,64–67] Moreover, several other hormones and transcription factors affect metabolic health (for example, IL-6, BDNF, Irisin,

BMPs, VEGF) and could contribute to improved glucose metabolism post-transplantation.[9,68–71] Therefore, it will be important to study the role of these factors as alternative mechanisms in future studies. It will also be interesting to see if additional stimulation of these cells prior to transplantation changes or improves their metabolic capacity.

One stimulus known to activate BAT is cold exposure.[2,72–74] Previous BAT transplantation studies observed improved thermogenic capacity in the recipients.[2,72,75,76] In our model, there was no effect of cell transplantation on cold tolerance, thermogenic activity, or thermogenic gene expression in WAT of recipient mice. This suggests that cell amount and/or innervation of transplanted cells or tissue might be vital to improve thermogenic capacity, and that beiging of WAT is likely not a contributing factor in the observed metabolic improvements post-transplant.

Data demonstrating that transplantation of human brown adipocytes in HFD-fed humanized mice improved glucose tolerance and insulin sensitivity up to 20 weeks post-transplantation suggest a potential therapeutic efficacy of the cells in type 2 diabetes. This logically leads to the important question of whether a practical means can be found for the manufacture of clinical-grade cells. This would require, among other criteria, a means of manufacturing the cells with a high degree of purity and scalability, a low cost of goods, cells modified to permit allogeneic transplantation, as well as an appropriate matrix under cGMP conditions. The isolation of human PSC-derived clonal progenitors such as the cell line NP88 utilized in this study may simplify quality control and reduce manufacturing costs since scale-up simply requires the serial expansion of the progenitors. However, additional studies will be required to optimize the dosage, the degree of cell differentiation prior to administration, transplantation matrix, site of transplantation, study the long-term viability of the cells, as well as extent of vascularization and innervation of the graft before definitive preclinical and clinical studies could commence. There is therefore a critical need for extensive research and development to fully evaluate this potential therapeutic modality and obtain the preclinical data required for human clinical trials.[77]

In summary, these data demonstrate the novel ability of a small number of committed brown adipocytes from BAT SVF or human stem cells to modulate metabolic health upon transplantation. They also establish an *in vivo* role for FGF21 to mediate these metabolic improvements, especially insulin sensitivity, differently in WT and FGF21$^{-/-}$ mice, through AKT signaling. This study identifies a role for committed brown adipocytes that when transplanted can improve glucose metabolism, even in small numbers. This could form the basis for a sustainable therapeutic strategy to improve metabolic health and mitigate obesity and type 2 diabetes in a human setting.

Limitations of the study

An important limitation of the study is the exclusive use of male donor and recipient mice. It is possible that brown adipocytes transplanted from or into female mice have a different effect on glucose homeostasis and insulin sensitivity. Furthermore, the activity of FGF21 could be altered in the presence of estradiol within adipose tissue. Other limitations include the potential role of other metabolic mediators, other recipient endogenous tissues, and the long-term traceability of transplanted cells. Future work will focus on addressing these limitations.

STAR★METHODS

Detailed methods are provided in the online version of this paper and include the following:

- KEY RESOURCES TABLE
- RESOURCE AVAILABILITY
  - Lead contact
  - Materials availability
  - Data and code availability
- EXPERIMENTAL MODEL AND STUDY PARTICIPANT DETAILS
  - Mouse models
- METHOD DETAILS
  - Isolation, culture, and differentiation of stromal vascular fraction from brown adipose tissue
  - Transplantation of cells into mice
  - Culture, differentiation, and transplantation of AgeX-NP88 human brown adipocytes (hBAs)
  - IVIS bioluminescent imaging
  - Body composition, glucose, and insulin tolerance tests
  - Cold tolerance test
  - qPCR
  - Western blotting
  - Acute insulin stimulation
  - ELISA
  - Cell imaging
- QUANTIFICATION AND STATISTICAL ANALYSIS
  - RNA sequencing analysis
  - Statistical analysis

SUPPLEMENTAL INFORMATION

Supplemental information can be found online at https://doi.org/10.1016/j.isci.2024.108927.

ACKNOWLEDGMENTS

This work was supported by National Institutes of Health grant K01-DK-105109 and R01-HL-138738 (to K.I.S.). P.V. was supported by an AHAPRE903654 Predoctoral Fellowship and F.Y. was supported by T32-HL134616. P.Y., E.P.-C., and H.W. were supported in part by National Institutes of Health grant P30-CA016058 for the services provided by OSU Comprehensive Cancer Center – Genomics Shared Resource.

AUTHOR CONTRIBUTIONS

This study was conceived and designed by K.I.S. and R.S.D. Experiments were carried out by R.S.D., F.T.Y., L.A.B., P.V., D.H.-S., N.P.S., O.T., and L.H. Scaffolds were generated and provided by M.K.D. and R.D.A. mRNA library generation and sequencing were carried out by P.Y., E.P.-C., and H.W. RNA sequencing analysis was carried out by R.S.D., A.G., and F.N. under the supervision of C.W. The human brown adipocyte AgeX-NP88 cell line was supplied by M.D.W., R.S., H.S., and N.N.M. (AgeX Therapeutics). R.S.D. and K.I.S. analyzed and interpreted the data. The manuscript was written by R.S.D. and K.I.S. with input from other authors. All authors gave final approval for publication.

DECLARATION OF INTERESTS

M.D.W., R.S., H.S., and N.N.M. are employed by AgeX Therapeutics.

Received: October 31, 2023
Revised: December 15, 2023
Accepted: January 12, 2024
Published: January 17, 2024

REFERENCES

1. https://www.who.int/en/news-room/fact-sheets/detail/obesity-and-overweight. https://www.who.int/en/news-room/fact-sheets/detail/obesity-and-overweight.
2. Stanford, K.I., Middelbeek, R.J.W., Townsend, K.L., An, D., Nygaard, E.B., Hitchcox, K.M., Markan, K.R., Nakano, K., Hirshman, M.F., Tseng, Y.H., and Goodyear, L.J. (2013). Brown adipose tissue regulates glucose homeostasis and insulin sensitivity. J. Clin. Invest. *123*, 215–223.
3. White, J.D., Dewal, R.S., and Stanford, K.I. (2019). The beneficial effects of brown adipose tissue transplantation. Mol. Aspect. Med. *68*, 74–81.
4. Gunawardana, S.C., and Piston, D.W. (2012). Reversal of type 1 diabetes in mice by brown adipose tissue transplant. Diabetes *61*, 674–682.
5. Gunawardana, S.C., and Piston, D.W. (2015). Insulin-independent reversal of type 1 diabetes in nonobese diabetic mice with brown adipose tissue transplant. Am. J. Physiol. Endocrinol. Metab. *308*, E1043–E1055.
6. Zhu, Z., Spicer, E.G., Gavini, C.K., Goudjo-Ako, A.J., Novak, C.M., and Shi, H. (2014). Enhanced sympathetic activity in mice with brown adipose tissue transplantation (transBATation). Physiol. Behav. *125*, 21–29.
7. Tran, T.T., and Kahn, C.R. (2010). Transplantation of adipose tissue and stem cells: role in metabolism and disease. Nat. Rev. Endocrinol. *6*, 195–213.
8. Silva, F.J., Holt, D.J., Vargas, V., Yockman, J., Boudina, S., Atkinson, D., Grainger, D.W., Revelo, M.P., Sherman, W., Bull, D.A., and Patel, A.N. (2014). Metabolically active human brown adipose tissue derived stem cells. Stem Cell. *32*, 572–581.
9. Elsen, M., Raschke, S., Tennagels, N., Schwahn, U., Jelenik, T., Roden, M., Romacho, T., and Eckel, J. (2014). BMP4 and BMP7 induce the white-to-brown transition of primary human adipose stem cells. Am. J. Physiol. Cell Physiol. *306*, C431–C440.
10. Wang, C.H., Lundh, M., Fu, A., Kriszt, R., Huang, T.L., Lynes, M.D., Leiria, L.O., Shamsi, F., Darcy, J., Greenwood, B.P., et al. (2020). CRISPR-engineered human brown-like adipocytes prevent diet-induced obesity and ameliorate metabolic syndrome in mice. Sci. Transl. Med. *12*, eaaz8664.
11. Dewal, R.S., and Stanford, K.I. (2019). Effects of exercise on brown and beige adipocytes. Biochim. Biophys. Acta Mol. Cell Biol. Lipids *1864*, 71–78.
12. Lee, D.V., Li, D., Yan, Q., Zhu, Y., Goodwin, B., Calle, R., Brenner, M.B., and Talukdar, S. (2014). Fibroblast growth factor 21 improves insulin sensitivity and synergizes with insulin in human adipose stem cell-derived (hASC) adipocytes. PLoS One *9*, e111767.
13. Li, H., Wu, G., Fang, Q., Zhang, M., Hui, X., Sheng, B., Wu, L., Bao, Y., Li, P., Xu, A., and Jia, W. (2018). Fibroblast growth factor 21 increases insulin sensitivity through specific expansion of subcutaneous fat. Nat. Commun. *9*, 272.
14. Lin, Z., Tian, H., Lam, K.S.L., Lin, S., Hoo, R.C.L., Konishi, M., Itoh, N., Wang, Y., Bornstein, S.R., Xu, A., and Li, X. (2013). Adiponectin Mediates the Metabolic Effects of FGF21 on Glucose Homeostasis and Insulin Sensitivity in Mice. Cell Metabol. *17*, 779–789.
15. Aalipour, A., Chuang, H.Y., Murty, S., D'Souza, A.L., Park, S.M., Gulati, G.S., Patel, C.B., Beinat, C., Simonetta, F., Martinić, I., et al. (2019). Engineered immune cells as highly sensitive cancer diagnostics. Nat. Biotechnol. *37*, 531–539.
16. Bi, Y., Zhang, N., and He, Y. (2022). Non-invasive In Vivo Tracking of Mammalian Cells Stably Expressing Firefly Luciferase. In Bioluminescence: Methods and Protocols, *Volume 1*, S.-B. Kim, ed (Springer US), pp. 299–306.
17. Gerace, D., Boulanger, K.R., Hyoje-Ryu Kenty, J., and Melton, D.A. (2021). Generation of a heterozygous GAPDH-Luciferase human ESC line (HVRDe008-A-1) for in vivo monitoring of stem cells and their differentiated progeny. Stem Cell Res. *53*, 102371.
18. Komatsu, H., Gonzalez, N., Ortiz, J., Rawson, J., Omori, K., Kandeel, F., and Mullen, Y. (2021). Early-Phase Luciferase Signals of Islet Grafts Predicts Successful Subcutaneous Site Transplantation in Rats. Mol. Imag. Biol. *23*, 173–179.
19. Schubert, R., Sann, J., Frueh, J.T., Ullrich, E., Geiger, H., and Baer, P.C. (2018). Tracking of Adipose-Derived Mesenchymal Stromal/Stem Cells in a Model of Cisplatin-Induced Acute Kidney Injury: Comparison of Bioluminescence Imaging versus qRT-PCR. Int. J. Mol. Sci. *19*, 2564.
20. Gray, C.W., and Coster, A.C.F. (2020). From insulin to Akt: Time delays and dominant processes. J. Theor. Biol. *507*, 110454.
21. Hernandez, R., Teruel, T., and Lorenzo, M. (2001). Akt mediates insulin induction of glucose uptake and up-regulation of GLUT4 gene expression in brown adipocytes. FEBS Lett. *494*, 225–231.
22. Sostre-Colón, J., Uehara, K., Garcia Whitlock, A.E., Gavin, M.J., Ishibashi, J., Potthoff, M.J., Seale, P., and Titchenell, P.M. (2021). Hepatic AKT orchestrates adipose tissue thermogenesis via FGF21-dependent and -independent mechanisms. Cell Rep. *35*, 109128.
23. Hui, X., Zhu, W., Wang, Y., Lam, K.S.L., Zhang, J., Wu, D., Kraegen, E.W., Li, Y., and Xu, A. (2009). Major urinary protein-1 increases energy expenditure and improves glucose

intolerance through enhancing mitochondrial function in skeletal muscle of diabetic mice. J. Biol. Chem. *284*, 14050–14057.
24. Zhou, Y., Jiang, L., and Rui, L. (2009). Identification of MUP1 as a regulator for glucose and lipid metabolism in mice. J. Biol. Chem. *284*, 11152–11159.
25. Luo, M., Mengos, A.E., Stubblefield, T.M., and Mandarino, L.J. (2012). High Fat Diet-Induced Changes in Hepatic Protein Abundance in Mice. J. Proteonomics Bioinf. *5*, 60–66.
26. Greve, S., Kuhn, G.A., Saenz-de-Juano, M.D., Ghosh, A., von Meyenn, F., and Giller, K. (2022). The major urinary protein gene cluster knockout mouse as a novel model for translational metabolism research. Sci. Rep. *12*, 13161.
27. Coskun, T., Bina, H.A., Schneider, M.A., Dunbar, J.D., Hu, C.C., Chen, Y., Moller, D.E., and Kharitonenkov, A. (2008). Fibroblast growth factor 21 corrects obesity in mice. Endocrinology *149*, 6018–6027.
28. Emanuelli, B., Vienberg, S.G., Smyth, G., Cheng, C., Stanford, K.I., Arumugam, M., Michael, M.D., Adams, A.C., Kharitonenkov, A., and Kahn, C.R. (2014). Interplay between FGF21 and insulin action in the liver regulates metabolism. J. Clin. Invest. *124*, 515–527.
29. Hanssen, M.J.W., Broeders, E., Samms, R.J., Vosselman, M.J., van der Lans, A.A.J.J., Cheng, C.C., Adams, A.C., van Marken Lichtenbelt, W.D., and Schrauwen, P. (2015). Serum FGF21 levels are associated with brown adipose tissue activity in humans. Sci. Rep. *5*, 10275.
30. Loyd, C., Magrisso, I.J., Haas, M., Balusu, S., Krishna, R., Itoh, N., Sandoval, D.A., Perez-Tilve, D., Obici, S., and Habegger, K.M. (2016). Fibroblast growth factor 21 is required for beneficial effects of exercise during chronic high-fat feeding. J. Appl. Physiol. *121*, 687–698.
31. Owen, B.M., Mangelsdorf, D.J., and Kliewer, S.A. (2015). Tissue-specific actions of the metabolic hormones FGF15/19 and FGF21. Trends Endocrinol. Metabol. *26*, 22–29.
32. Adams, A.C., Halstead, C.A., Hansen, B.C., Irizarry, A.R., Martin, J.A., Myers, S.R., Reynolds, V.L., Smith, H.W., Wroblewski, V.J., and Kharitonenkov, A. (2013). LY2405319, an Engineered FGF21 Variant, Improves the Metabolic Status of Diabetic Monkeys. PLoS One *8*, e65763.
33. Benomar, Y., Amine, H., Crépin, D., Al Rifai, S., Riffault, L., Gertler, A., and Taouis, M. (2016). Central Resistin/TLR4 Impairs Adiponectin Signaling, Contributing to Insulin and FGF21 Resistance. Diabetes *65*, 913–926.
34. BonDurant, L.D., Ameka, M., Naber, M.C., Markan, K.R., Idiga, S.O., Acevedo, M.R., Walsh, S.A., Ornitz, D.M., and Potthoff, M.J. (2017). FGF21 Regulates Metabolism Through Adipose-Dependent and -Independent Mechanisms. Cell Metabol. *25*, 935–944.e4.
35. Holland, W.L., Adams, A.C., Brozinick, J.T., Bui, H.H., Miyauchi, Y., Kusminski, C.M., Bauer, S.M., Wade, M., Singhal, E., Cheng, C.C., et al. (2013). An FGF21-adiponectin-ceramide axis controls energy expenditure and insulin action in mice. Cell Metabol. *17*, 790–797.
36. Hui, X., Feng, T., Liu, Q., Gao, Y., and Xu, A. (2016). The FGF21–adiponectin axis in controlling energy and vascular homeostasis. J. Mol. Cell Biol. *8*, 110–119.
37. Liu, Y., Palanivel, R., Rai, E., Park, M., Gabor, T.V., Scheid, M.P., Xu, A., and Sweeney, G. (2015). Adiponectin Stimulates Autophagy and Reduces Oxidative Stress to Enhance Insulin Sensitivity During High-Fat Diet Feeding in Mice. Diabetes *64*, 36–48.
38. Talukdar, S., Zhou, Y., Li, D., Rossulek, M., Dong, J., Somayaji, V., Weng, Y., Clark, R., Lanba, A., Owen, B.M., et al. (2016). A Long-Acting FGF21 Molecule, PF-05231023, Decreases Body Weight and Improves Lipid Profile in Non-human Primates and Type 2 Diabetic Subjects. Cell Metabol. *23*, 427–440.
39. So, W.Y., Cheng, Q., Xu, A., Lam, K.S.L., and Leung, P.S. (2015). Loss of fibroblast growth factor 21 action induces insulin resistance, pancreatic islet hyperplasia and dysfunction in mice. Cell Death Dis. *6*, e1707.
40. Porter, J.W., Rowles, J.L., Fletcher, J.A., Zidon, T.M., Winn, N.C., McCabe, L.T., Park, Y.-M., Perfield, J.W., Thyfault, J.P., Rector, R.S., et al. (2017). Anti-inflammatory effects of exercise training in adipose tissue do not require FGF21. J. Endocrinol. *235*, 97–109.
41. Cook, S.A., Varela-Carver, A., Mongillo, M., Kleinert, C., Khan, M.T., Leccisotti, L., Strickland, N., Matsui, T., Das, S., Rosenzweig, A., et al. (2010). Abnormal myocardial insulin signalling in type 2 diabetes and left-ventricular dysfunction. Eur. Heart J. *31*, 100–111.
42. Landa-Galvan, H.V., Rios-Castro, E., Romero-Garcia, T., Rueda, A., and Olivares-Reyes, J.A. (2020). Metabolic syndrome diminishes insulin-induced Akt activation and causes a redistribution of Akt-interacting proteins in cardiomyocytes. PLoS One *15*, e0228115.
43. Abel, E.D., O'Shea, K.M., and Ramasamy, R. (2012). Insulin resistance: metabolic mechanisms and consequences in the heart. Arterioscler. Thromb. Vasc. Biol. *32*, 2068–2076.
44. Hendley, M.A., Isely, C., Murphy, K.P., Hall, H.E., Annamalai, P., and Gower, R.M. (2020). Scaffold Implant Into the Epididymal Adipose Tissue Protects Mice From High Fat Diet Induced Ectopic Lipid Accumulation and Hyperinsulinemia. Front. Bioeng. Biotechnol. *8*, 562.
45. Chen, L., Wang, L., Li, Y., Wuang, L., Liu, Y., Pang, N., Luo, Y., He, J., Zhang, L., Chen, N., et al. (2018). Transplantation of Normal Adipose Tissue Improves Blood Flow and Reduces Inflammation in High Fat Fed Mice With Hindlimb Ischemia. Front. Physiol. *9*, 197.
46. Fukumura, D., Ushiyama, A., Duda, D.G., Xu, L., Tam, J., Krishna, V., Chatterjee, K., Garkavtsev, I., and Jain, R.K. (2003). Paracrine regulation of angiogenesis and adipocyte differentiation during in vivo adipogenesis. Circ. Res. *93*, e88–e97.
47. Mandrup, S., Loftus, T.M., MacDougald, O.A., Kuhajda, F.P., and Lane, M.D. (1997). Obese gene expression at in vivo levels by fat pads derived from s.c. implanted 3T3-F442A preadipocytes. Proc. Natl. Acad. Sci. USA *94*, 4300–4305.
48. Nishio, M., Yoneshiro, T., Nakahara, M., Suzuki, S., Saeki, K., Hasegawa, M., Kawai, Y., Akutsu, H., Umezawa, A., Yasuda, K., et al. (2012). Production of Functional Classical Brown Adipocytes from Human Pluripotent Stem Cells using Specific Hemopoietin Cocktail without Gene Transfer. Cell Metabol. *16*, 394–406.
49. Ogihara, Y., Yukawa, H., Kameyama, T., Nishi, H., Onoshima, D., Ishikawa, T., Torimoto, T., and Baba, Y. (2017). Labeling and in vivo visualization of transplanted adipose tissue-derived stem cells with safe cadmium-free aqueous ZnS coating of ZnS-AgInS2 nanoparticles. Sci. Rep. *7*, 40047.
50. Rieck, B., and Schlaak, S. (2003). In Vivo Tracking of Rat Preadipocytes After Autologous Transplantation. Ann. Plast. Surg. *51*, 294–300.
51. Schreiter, J.S., Kurow, L.O., Langer, S., Steinert, M., and Massier, L. (2021). Effects of non-vascularized adipose tissue transplantation on its genetic profile. Adipocyte *10*, 131–141.
52. Shibasaki, M., Takahashi, K., Itou, T., Miyazawa, S., Ito, M., Kobayashi, J., Bujo, H., and Saito, Y. (2002). Alterations of insulin sensitivity by the implantation of 3T3-L1 cells in nude mice. A role for TNF-α? Diabetologia *45*, 518–526.
53. Xue, S., Wu, G., Zhang, H.-t., Guo, Y.-w., Zou, Y.-x., Zhou, Z.-j., Jiang, X.-d., Ke, Y.-q., and Xu, R.-x. (2015). Transplantation of Adipocyte-Derived Stem Cells in a Hydrogel Scaffold for the Repair of Cortical Contusion Injury in Rats. J. Neurotrauma *32*, 506–515.
54. Badman, M.K., Koester, A., Flier, J.S., Kharitonenkov, A., and Maratos-Flier, E. (2009). Fibroblast growth factor 21-deficient mice demonstrate impaired adaptation to ketosis. Endocrinology *150*, 4931–4940.
55. Izumiya, Y., Bina, H.A., Ouchi, N., Akasaki, Y., Kharitonenkov, A., and Walsh, K. (2008). FGF21 is an Akt-regulated myokine. FEBS Lett. *582*, 3805–3810.
56. Makarova, E., Kazantseva, A., Dubinina, A., Jakovleva, T., Balybina, N., Baranov, K., and Bazhan, N. (2021). The Same Metabolic Response to FGF21 Administration in Male and Female Obese Mice Is Accompanied by Sex-Specific Changes in Adipose Tissue Gene Expression. Int. J. Mol. Sci. *22*, 10561.
57. Challa, T.D., Dapito, D.H., Kulenkampff, E., Kiehlmann, E., Moser, C., Straub, L., Sun, W., and Wolfrum, C. (2020). A Genetic Model to Study the Contribution of Brown and Brite Adipocytes to Metabolism. Cell Rep. *30*, 3424–3433.e4.
58. Thompson, W.C., Zhou, Y., Talukdar, S., and Musante, C.J. (2016). PF-05231023, a long-acting FGF21 analogue, decreases body weight by reduction of food intake in non-human primates. J. Pharmacokinet. Pharmacodyn. *43*, 411–425.
59. Kharitonenkov, A., Beals, J.M., Micanovic, R., Strifler, B.A., Rathnachalam, R., Wroblewski, V.J., Li, S., Koester, A., Ford, A.M., Coskun, T., et al. (2013). Rational design of a fibroblast growth factor 21-based clinical candidate, LY2405319. PLoS One *8*, e58575.
60. Kharitonenkov, A., Wroblewski, V.J., Koester, A., Chen, Y.F., Clutinger, C.K., Tigno, X.T., Hansen, B.C., Shanafelt, A.B., and Etgen, G.J. (2007). The metabolic state of diabetic monkeys is regulated by fibroblast growth factor-21. Endocrinology *148*, 774–781.
61. Hecht, R., Li, Y.S., Sun, J., Belouski, E., Hall, M., Hager, T., Yie, J., Wang, W., Winters, D., Smith, S., et al. (2012). Rationale-Based Engineering of a Potent Long-Acting FGF21 Analog for the Treatment of Type 2 Diabetes. PLoS One *7*, e49345.
62. Chang, L., Chiang, S.-H., and Saltiel, A.R. (2004). Insulin Signaling and the Regulation of Glucose Transport. Mol. Med. *10*, 65–71.
63. Pinckard, K.M., Shettigar, V.K., Wright, K.R., Abay, E., Baer, L.A., Vidal, P., Dewal, R.S., Das, D., Duarte-Sanmiguel, S., Hernández-Saavedra, D., et al. (2021). A Novel Endocrine Role for the BAT-Released Lipokine

12,13-diHOME to Mediate Cardiac Function. Circulation *143*, 145–159.
64. Kharitonenkov, A., Shiyanova, T.L., Koester, A., Ford, A.M., Micanovic, R., Galbreath, E.J., Sandusky, G.E., Hammond, L.J., Moyers, J.S., Owens, R.A., et al. (2005). FGF-21 as a novel metabolic regulator. J. Clin. Invest. *115*, 1627–1635.
65. Shamsi, F., Xue, R., Huang, T.L., Lundh, M., Liu, Y., Leiria, L.O., Lynes, M.D., Kempf, E., Wang, C.-H., Sugimoto, S., et al. (2020). FGF6 and FGF9 regulate UCP1 expression independent of brown adipogenesis. Nat. Commun. *11*, 1421.
66. Hondares, E., Iglesias, R., Giralt, A., Gonzalez, F.J., Giralt, M., Mampel, T., and Villarroya, F. (2011). Thermogenic activation induces FGF21 expression and release in brown adipose tissue. J. Biol. Chem. *286*, 12983–12990.
67. Huang, Z., Tan, Y., Gu, J., Liu, Y., Song, L., Niu, J., Zhao, L., Srinivasan, L., Lin, Q., Deng, J., et al. (2017). Uncoupling the Mitogenic and Metabolic Functions of FGF1 by Tuning FGF1-FGF Receptor Dimer Stability. Cell Rep. *20*, 1717–1728.
68. Lee, P., Linderman, J.D., Smith, S., Brychta, R.J., Wang, J., Idelson, C., Perron, R.M., Werner, C.D., Phan, G.Q., Kammula, U.S., et al. (2014). Irisin and FGF21 are cold-induced endocrine activators of brown fat function in humans. Cell Metabol. *19*, 302–309.
69. Boström, P., Wu, J., Jedrychowski, M.P., Korde, A., Ye, L., Lo, J.C., Rasbach, K.A., Boström, E.A., Choi, J.H., Long, J.Z., et al. (2012). A PGC1-α-dependent myokine that drives brown-fat-like development of white fat and thermogenesis. Nature *481*, 463–468.
70. Cao, L., Choi, E.Y., Liu, X., Martin, A., Wang, C., Xu, X., and During, M.J. (2011). White to brown fat phenotypic switch induced by genetic and environmental activation of a hypothalamic-adipocyte axis. Cell Metabol. *14*, 324–338.
71. Tobin, J.F., and Celeste, A.J. (2006). Bone morphogenetic proteins and growth differentiation factors as drug targets in cardiovascular and metabolic disease. Drug Discov. Today *11*, 405–411.
72. Peres Valgas da Silva, C., Hernández-Saavedra, D., White, J.D., and Stanford, K.I. (2019). Cold and Exercise: Therapeutic Tools to Activate Brown Adipose Tissue and Combat Obesity. Biology *8*, 9.
73. Saito, M., Okamatsu-Ogura, Y., Matsushita, M., Watanabe, K., Yoneshiro, T., Nio-Kobayashi, J., Iwanaga, T., Miyagawa, M., Kameya, T., Nakada, K., et al. (2009). High incidence of metabolically active brown adipose tissue in healthy adult humans: effects of cold exposure and adiposity. Diabetes *58*, 1526–1531.
74. van Marken Lichtenbelt, W.D., Vanhommerig, J.W., Smulders, N.M., Drossaerts, J.M.A.F.L., Kemerink, G.J., Bouvy, N.D., Schrauwen, P., and Teule, G.J.J. (2009). Cold-activated brown adipose tissue in healthy men. N. Engl. J. Med. *360*, 1500–1508.
75. Lidell, M.E. (2019). Brown Adipose Tissue in Human Infants. Handb. Exp. Pharmacol. *251*, 107–123.
76. Enerbäck, S., Jacobsson, A., Simpson, E.M., Guerra, C., Yamashita, H., Harper, M.E., and Kozak, L.P. (1997). Mice lacking mitochondrial uncoupling protein are cold-sensitive but not obese. Nature *387*, 90–94.
77. Zhu, T., Chen, X., and Jiang, S. (2023). Progress and obstacles in transplantation of brown adipose tissue or engineered cells with thermogenic potential for metabolic benefits. Front. Endocrinol. *14*, 1191278.
78. Chen, S. (2023). Ultrafast one-pass FASTQ data preprocessing, quality control, and deduplication using fastp. iMeta *2*, e107.
79. Bray, N.L., Pimentel, H., Melsted, P., and Pachter, L. (2016). Near-optimal probabilistic RNA-seq quantification. Nat. Biotechnol. *34*, 525–527.
80. Yu, G., Wang, L.G., Han, Y., and He, Q.Y. (2012). clusterProfiler: an R package for comparing biological themes among gene clusters. OMICS *16*, 284–287.
81. Schneider, C.A., Rasband, W.S., and Eliceiri, K.W. (2012). NIH Image to ImageJ: 25 years of image analysis. Nat. Methods *9*, 671–675.
82. Lehnig, A.C., Dewal, R.S., Baer, L.A., Kitching, K.M., Munoz, V.R., Arts, P.J., Sindeldecker, D.A., May, F.J., Lauritzen, H.P.M.M., Goodyear, L.J., and Stanford, K.I. (2019). Exercise Training Induces Depot-Specific Adaptations to White and Brown Adipose Tissue. iScience *11*, 425–439.
83. Rockwood, D.N., Preda, R.C., Yücel, T., Wang, X., Lovett, M.L., and Kaplan, D.L. (2011). Materials fabrication from Bombyx mori silk fibroin. Nat. Protoc. *6*, 1612–1631.
84. Stanford, K.I., Middelbeek, R.J.W., Townsend, K.L., Lee, M.Y., Takahashi, H., So, K., Hitchcox, K.M., Markan, K.R., Hellbach, K., Hirshman, M.F., et al. (2015). A novel role for subcutaneous adipose tissue in exercise-induced improvements in glucose homeostasis. Diabetes *64*, 2002–2014.
85. Shi, H., Bowers, R.R., and Bartness, T.J. (2004). Norepinephrine turnover in brown and white adipose tissue after partial lipectomy. Physiol. Behav. *81*, 535–542.
86. Tran, T.T., Yamamoto, Y., Gesta, S., and Kahn, C.R. (2008). Beneficial effects of subcutaneous fat transplantation on metabolism. Cell Metabol. *7*, 410–420.
87. Dewal, R.S., Greer-Short, A., Lane, C., Nirengi, S., Manzano, P.A., Hernández-Saavedra, D., Wright, K.R., Nassal, D., Baer, L.A., Mohler, P.J., et al. (2021). Phospho-ablation of cardiac sodium channel Na(v)1.5 mitigates susceptibility to atrial fibrillation and improves glucose homeostasis under conditions of diet-induced obesity. Int. J. Obes. *45*, 795–807.
88. Chen, S., Zhou, Y., Chen, Y., and Gu, J. (2018). fastp: an ultra-fast all-in-one FASTQ preprocessor. Bioinformatics *34*, i884–i890.
89. Love, M.I., Huber, W., and Anders, S. (2014). Moderated estimation of fold change and dispersion for RNA-seq data with DESeq2. Genome Biol. *15*, 550.
90. Wu, T., Hu, E., Xu, S., Chen, M., Guo, P., Dai, Z., Feng, T., Zhou, L., Tang, W., Zhan, L., et al. (2021). clusterProfiler 4.0: A universal enrichment tool for interpreting omics data. Innovation *2*, 100141.

STAR★METHODS

KEY RESOURCES TABLE

REAGENT or RESOURCE	SOURCE	IDENTIFIER
Antibodies		
AKT	CST	Cat #4691S
p-AKT	CST	Cat #S473
AMPK	CST	Cat #2532S
p-AMPK	CST	Cat #2535S
MUP1	Abcam	Cat #ab95198
MUP11	Thermo Fisher Scientific	Cat #PIPA5112879
MUP12	Thermo Fisher Scientific	Cat #NB125147
GAPDH	CST	Cat #2118S
p-AKT	CST	Cat #S473
AMPK	CST	Cat #2532S
p-AMPK	CST	Cat #2535S
MUP1	Abcam	Cat #ab95198
MUP11	Thermo Fisher Scientific	Cat #PIPA5112879
MUP12	Thermo Fisher Scientific	Cat #NB125147
GAPDH	CST	Cat #2118S
Chemicals, peptides, and recombinant proteins		
High-fat diet (60% kcal from Fat)	Research Diets Inc.	Cat #D12492i
IVISbrite D-Luciferin	Revvity	Cat #770504
Humulin-R	NDC	Cat #0002-8215-17 (HI-213)
Insulin, Cell culture	Roche	Cat #11376497001
Dextrose Anydrous	VWR	Cat #BDH9230
Qiazol	Qiagen	Cat #79306
DMEM Low Glucose	Invitrogen	Cat #11885-084
DMEM High Glucose	Thermo Fisher Scientific	Cat #1960-069
Dexamethasone	Sigma	Cat #D-4902
Fetal Bovine Serum	Corning	Cat #35-010-CV
ITS mix	Sigma	Cat #I3146
Indomethacin	Sigma	Cat #I7378
Linoleic-acid Albumin	Sigma	Cat #L9530
L-Ascorbic Acid Phosphate	Sigma	Cat #A8960
IBMX	Sigma	Cat #I5879
Penicillin/Streptomycin	Gibco	Cat #504284
Trypsin EDTA 0.25%	VWR	Cat #02-0154-0100
PBS	VWR	Cat #E504
Smooth Muscle Cell Growth Medium 2 and its Supplement Mix	Promocell	Cat #C-22062
Pyruvate	Gibco	Cat #11360
Glutamax	Gibco	Cat #35050
L-Proline	Sigma	Cat #D49752
T3	Sigma	Cat #T6397
Rosiglitazone	Sigma	Cat #R2408-10MG

(*Continued on next page*)

Continued

REAGENT or RESOURCE	SOURCE	IDENTIFIER
TrypLE Express Enzyme (1X), phenol	Thermo Fisher Scientific	Cat #12605010
Critical commercial assays		
Insulin ELISA	Millipore	Cat #EZRMI-13K
Adiponectin ELISA	Sigma	Cat #RAB1115-1KT
FGF21 ELISA	BioVendor R&D	Cat #RD291108200R
Qiagen RNeasy Plus Mini Kit	Qiagen	Cat #74134
Agilent BioAnalyzer RNA Nano Kit	Agilent Technologies	Cat #5067-1511
Invitrogen Qubit RNA HS Assay Kit	Thermo Fisher Scientific	Cat #Q32852
NEBNext Ultra II Directional RNA Library Prep Kit	NEB	Cat #E7760L
NEBNext Poly (A) mRNA Magnetic Isolation Module	NEB	Cat #E7490
Agilent BioAnalyzer HS DNA Kit	Agilent	Cat #5067-4626
Invitrogen Qubit DNA HS Assay Kit	Thermo Fisher Scientific	Cat #Q32854
Deposited data		
Bulk RNA-sequencing data (Liver)	Submitted on NCBI GEO database (https://www.ncbi.nlm.nih.gov/geo/)	Accession number: GSE250078
Experimental models: Cell lines		
AgeX-NP88 cell line	AgeX Therapeutics	Not Applicable
Experimental models: Organisms/strains		
FGF21 Knock-out mice	Jackson Laboratory	B6.129Sv(Cg)-Fgf21tm1.1Djm/
Wild-type mice	Charles River laboratories	C57BL/6J
Luciferase Transgenic mice	Jackson Laboratory	FVB-Tg [CAG-luc,-GFP] L2G85Chco/J
NSG mice	Jackson Laboratory	NOD.Cg-Prkdcscid Il2rgtm1Wjl/SzJ
Oligonucleotides		
Oligonucleotides	This paper: Table S1	
Software and algorithms		
GraphPad Prism 7	GraphPad Software	https://www.graphpad.com
R version 4.2.2	R Development Core Team, 2011	https://www.r-project.org/
Fastp version 0.20.0	Shifu Chen	Shifu Chen. 2023. Ultrafast one-pass FASTQ data preprocessing, quality control, and deduplication using fastp. iMeta 2: e107. https://doi.org/10.1002/imt2.107[78]
Kallisto version 0.46.1	Pachter Lab	Nicolas L Bray, Harold Pimentel, Páll Melsted and Lior Pachter, Near-optimal probabilistic RNA-seq quantification, Nature Biotechnology **34**, 525–527 (2016), https://doi.org/10.1038/nbt.3519[79]
clusterProfiler version 4.6.0	Guangchuang Yu	Yu G, Wang L, Han Y and He Q*. clusterProfiler: an R package for comparing biological themes among gene clusters. ***OMICS: A Journal of Integrative Biology***. 2012, 16(5):284-287[80]
Image J	NIH	Rasband, W.S., ImageJ, U. S. National Institutes of Health, Bethesda, Maryland, USA, https://imagej.net/ij/, 1997-2018.[81]

RESOURCE AVAILABILITY

Lead contact

Further information and requests for resources and reagents should be directed to and will be fulfilled by the lead contact, Dr. Kristin Stanford (kristin.stanford@osumc.edu).

Materials availability

This study did not generate unique reagents.

Data and code availability

- RNA-sequencing data that support the findings of this study have been deposited in the NCBI GEO database, with the accession code GSE250078 and are publicly available at the time of publication. The accession number is also listed in the key resources table.
- Original western blot images are available in a separate supplemental file 'Data S1'. Additional microscopy information will be shared by the lead contact upon request. This paper does not report original code.
- Any additional information required to reanalyze the data reported in this paper is available from the lead contact upon request.

EXPERIMENTAL MODEL AND STUDY PARTICIPANT DETAILS

Mouse models

Six-week-old C57BL/6J (WT) (Charles River Laboratories), FGF21$^{-/-}$ (B6.129Sv(Cg)-Fgf21tm1.1Djm/ Jackson Laboratory), or NSG (NOD.Cg-Prkdcscid Il2rgtm1Wjl/SzJ, Jackson Laboratories) male mice were used as recipients for the cell transplantation. Recipient mice were placed on a high-fat diet (60% kcal from fat) (Research Diets Inc.) for 6 weeks prior to transplantation and continued the HFD for 12 weeks post transplantation; NSG mice were maintained on a high-fat diet for 20 wks post-transplantation. Chow-fed 24- to 26-week-old untreated C57BL/6 male mice were used as age-matched controls for metabolic experiments. Donor mice were 10–12-week-old, C56BL/6 (WT), FGF21$^{-/-}$, or Luciferase transgenic (Luc tg; FVB-Tg [CAG-luc,-GFP] L2G85Chco/J from Jackson Laboratory) male mice that were chow-fed [standard mouse diet (21% kcal from fat) (9F 5020 Lab Diet, PharmaServ Inc.)]. For the NSG recipient mice, 2 or 4 million human brown adipocytes (hBAs) from the AgeX-NP88 line were used for transplantation. All animals were maintained on a standard 12-hour light/12-hour dark cycle. All procedures were conducted in accordance with the Guide for the Care and Use of Laboratory Animals published by the National Institutes of Health following protocols approved by the IACUC at The Ohio State University. Animals were euthanized using isoflurane and cervical dislocation followed by collection of tissue or cell isolation.

Due to significant variation in cell availability from WT and FGF21$^{-/-}$ donor mice, there was significant diversity in the number of mice used in each *in vivo* experiment. The Sham-WT group had the most variability with 6-46 mice depending on the type of experiment or analyses. All other groups had a sample size in the range of 5-15 per group for *in vivo* experimentation. No mice were removed from the study and the sample sizes for each experiment are specified in Figure Legends.

METHOD DETAILS

Isolation, culture, and differentiation of stromal vascular fraction from brown adipose tissue

Brown adipose tissue was excised from the interscapular region (iBAT) of 10–12-week-old male C57BL/6 mice. SVF was isolated as previously described.[82] Briefly, excised BAT is minced and placed into a shaking water bath at 37°C, in DMEM (1g/L Glucose) with 3.5% BSA and 100mg/50mL of Collagenase, Type 1, until the tissue is completely dissociated. This is followed by sequential centrifugation and filtration steps to remove other cell types and debris, resulting in a pellet of the stromal vascular fraction. After isolation, cells were plated at 1 million seeding density/ dish into sterile, culture-treated 10cm dishes. Once the cells reached 80-90% confluence, they were differentiated as previously described.[82] Briefly, cells were differentiated for up to 8 days using Adipogenic Induction Media (AIM) consisting of low glucose DMEM supplemented with 2% Fetal Bovine Serum, 10mg/ml Insulin, 1X ITS Mix, 1X Linoleic Acid-Albumin, 50mM L-Ascorbic Acid Phosphate, 30mM Indomethacin, 10μM T3, 5mM Dexamethasone and 5mM 3-isobutyl-1-methylxanthine (IBMX).

Transplantation of cells into mice

Pre-adipocytes were cultured and differentiated prior to transplantation. On the day of transplantation, cells were washed with PBS and trypsinized using 1.5ml Trypsin-EDTA/ 10cm dish. The trypsin was neutralized using media containing FBS, cells were collected in 50ml Falcon tubes and centrifuged into a pellet at 1200rpm for 12 minutes. The cell pellet was re-suspended in 1-5 ml of media and counted.

Transplantation of cells was performed using inert, silk scaffolds to mimic a 3D tissue environment. Silk scaffolds were prepared following established protocols.[83] Briefly, silk cocoons were degummed by boiling in a 0.02 M aqueous solution of sodium carbonate for 30 min. The remaining fibers dried overnight and were then dissolved in 9.3 M lithium bromide at 60°C for 4 hours. The resulting solution was dialyzed in milli-Q water for 48 hours with a total of 6 water changes. The solution was centrifuged twice at 4800 rpm at 4°C for 20 minutes to remove debris. The resulting silk solution was lyophilized. To form silk scaffolds, the lyophilized silk was dissolved in hexafluoroisopropanol (HFIP) overnight to generate a 17% silk solution. The solution was poured over sodium chloride crystals with diameters between 500 and 600 μm. The containers were sealed for 24 hours and then opened to allow the HFIP to evaporate for 24 hours. Following evaporation, the scaffolds were placed in methanol for 24 hours to induce beta-sheet formation and the scaffolds were dried in the fume hood for 24 hours. To remove the salt porogen, scaffolds were rinsed in milli-Q water for 2–-3 days. Finally, the scaffolds were cut into cylinders of 2 mm height and 4 mm diameter.

Each scaffold can accommodate a maximum of 1 million cells. Twenty-four hours prior to transplantation the scaffolds were autoclaved in Molecular Grade Water and suspended in AIM in a CO_2 incubator at 37°C overnight. Committed pre-adipocytes on day 3 of differentiation

were trypsinized and counted as described above. Committed pre-adipocytes were re-suspended at concentrations of 1 million cells in 10μl of differentiation media, and 5μl of the suspension was slowly added on top of one scaffold. The cells were allowed to percolate through the scaffold following which the scaffold was inverted and the remaining 5μl suspension was added on the other side. Committed pre-adipocytes were allowed to incubate and attach to scaffolds for 2 hours in a CO_2 incubator at 37°C and then transplanted into the visceral cavity of recipient mice. A subset of transplantations were carried out using isolated, undifferentiated SVF cells. These cells were placed directly onto the scaffolds after isolation and allowed to attach for 2 hours in a CO_2 incubator at 37°C, followed by transplantation as described below.

High-fat diet (HFD) fed recipient mice were anesthetized by isoflurane inhalation in oxygen (3% isoflurane in 97% oxygen). For each recipient mouse, 1 million (1 scaffold) or 2 million (2 scaffolds) SVF cells or committed pre-adipocytes were transplanted into the visceral cavity. The perigonadal fat pad was visualized and scaffolds were carefully placed near it as previously described.[2,84–86] Mice that were sham operated (Sham-WT or Sham-KO) underwent the same procedure but received empty scaffolds. NSAIDs were not used during transplantation surgery to prevent interference with metabolic outcomes. The use of minimal analgesics does not affect survival, recovery, body mass, food intake, or inflammatory markers as seen in our previous studies.[2,84–86]

Culture, differentiation, and transplantation of AgeX-NP88 human brown adipocytes (hBAs)

Cells from the AgeX-NP88 cell line were derived from the human ES cell line 'Envy', which is a GFP-modified hES3. These cells, stored in liquid nitrogen, were thawed briefly, and grown using Smooth Muscle Cell Growth Medium 2 and its Supplement mix with 0.1% Gelatin coating in T-225 flasks. Upon reaching 80% confluence cells were split using TrypLE, transferred to 10cm dishes, and grown until confluency. A subset of cells were frozen in ice cold 90% FBS + 10% DMSO and stored in liquid nitrogen. Upon confluency, cells were differentiated for up to 10 days in serum-free DMEM (Glucose 4.5g/dL) media supplemented with 1mM Pyruvate, 2mM Glutamax, 0.1μM Dexamethasone, 0.35mM L-Proline, 0.17mM 2-phospho-L-Ascorbic Acid, ITS supplement, 2nM T3 and 1uM Rosiglitazone.

On day 3 of differentiation, cells were washed with PBS, trypsinized using TrypLE and transferred onto silk scaffolds as described in section 2.3. Silk scaffolds containing 2 or 4 million human brown adipocytes (hBAs), and empty silk scaffolds as controls (Sham) were then transplanted into HFD-fed, immunodeficient NSG male mice using the transplantation protocol described in section 2.3.

IVIS bioluminescent imaging

3D silk scaffolds containing committed pre-adipocytes from LucTg donors were incubated with 50μl Luciferin or transplanted into 6-week-old C57BL/6J recipient male mice. Mice that received cells from LucTg mice were injected with 150 mg Luciferin/kg body weight (D-Luciferin; Revvity Cat # 770505). Scaffolds incubated with, or mice injected with Luciferin were imaged using the IVIS Bioluminescent imaging software. Images were taken at 3-minute exposures for 30 minutes using the open filter and compiled within the IVIS imaging software.

Body composition, glucose, and insulin tolerance tests

Body weight was measured using an OHAUS NV212 scale. Body fat and lean mass were measured using an EchoMRI instrument (EchoMRI LLC) with canola oil calibration. Glucose tolerance testing was performed after a 12-h fast with drinking water available *ad libitum*. Blood glucose was assessed at baseline by a tail vein prick. Glucose was administered by intraperitoneal injection (2 g glucose/kg body weight) at 0 min, and the tail vein prick was used to measure blood glucose levels at 15, 30, 60, and 120 min post injection.[2] Insulin tolerance testing was performed following a 2 h fast with drinking water *ad libitum*. Baseline blood glucose levels were measured using a tail vein prick. Insulin was administered by intraperitoneal injection (1 unit per kg body weight) at 0 min. Blood glucose levels were measured at 10, 15, 30, 45, and 60 min post injection.[2] If at any time a mouse dropped below 40 mg/dL glucose, they were given an intraperitoneal injection of 200 μL of 20% glucose (0.2 g/mL) and subsequently removed from the test.[2] Glucose concentrations were determined from blood using a OneTouch Ultra-portable glucometer (LifeScan, Milpitas, CA).

Cold tolerance test

Mice were fasted for 4 hours (6am to 10am) and baseline rectal temperature was measured using an animal rectal probe thermometer (Physitemp). Mice were individually housed and placed in a thermal incubator at 4°C for 4 hours and rectal temperature was measured 30, 60, 120, 180 and 240 minutes after start of cold exposure.

qPCR

Pre-adipocytes from BAT SVF and brown adipocytes from the AgeX-NP88 line (On days 0, 1, 3, 5, 7, 8 or 10 post-differentiation), as well as recipient tissues were incubated with QIAzol and RNA was extracted using phenol-chloroform extraction. Cell and tissue processing and quantitative PCR (qPCR) were performed as previously described.[87] Briefly, the tissue was flash frozen and stored at −80 °C until processing. mRNA was measured by qRT-PCR (Roche LightCycler 480II) using SYBR Green detection (QuantaBio). Sigma-Aldrich custom primers were used for genes of interest with the sequences shown in Table S1. All qPCR genes were normalized to the housekeeping genes GAPDH or Beta-actin.

Western blotting

Tissue processing and immunoblotting were performed as previously described.[82] AKT (CST #4691S), p-AKT (CST #S473), AMPK (CST #2532S), p-AMPK (CST #2535S), MUP1 (Abcam #ab95198), MUP11 (Thermo Fisher Scientific #PIPA5112879), MUP12 (Thermo Fisher Scientific #NB125147) were used. Phosphorylated antibodies were normalized against total antibody concentration, which were normalized to GAPDH (CST #2118S). Images were analyzed using ImageJ (NIH; https://imagej.net/ij/ij/).

Acute insulin stimulation

In a subset of mice, insulin was administered by intraperitoneal injection (1 unit per kg body weight) 15 minutes prior to tissue collection. Tissue processing and immunoblotting were performed as described in the section titled 'Western blotting'.

ELISA

Blood was collected in anesthetized mice via cardiac puncture and after an overnight fast. Plasma insulin (Millipore), Adiponectin (Sigma) and FGF21 (BioVendor R&D) were measured using mouse ELISA kits.

Cell imaging

Microscopic imaging of adipocytes was carried out using the REVOLVE invertible microscope under visible light at 10x, 20x or 40x magnifications.

QUANTIFICATION AND STATISTICAL ANALYSIS

RNA sequencing analysis

A. Total RNA extraction and input RNA assessment

Total RNA was extracted from liver tissues using the Qiagen RNeasy Plus Mini Kit. The RNA Integrity Number (RIN) for total RNA were assessed using Agilent BioAnalyzer RNA Nano Kit (#5067-1511; Agilent Technologies, Inc., Santa Clara, CA) and the RNA amount were assayed with the Invitrogen Qubit RNA HS Assay Kit (#Q32852; Thermo Fisher Scientific, Waltham, MA).

B. mRNA-seq library generation, sequencing, and analysis

Samples with RIN > 7 were used in mRNA-seq library generation using the NEBNext® Ultra™ II Directional (stranded) RNA Library Prep Kit (#E7760L; Ipswich, MA) plus the NEBNext Poly (A) mRNA Magnetic Isolation Module (#E7490). Briefly, 200 ng total RNA were used as input. RNA fragmentation was set at 10 minutes and 12 PCR cycles were used in final library generation. Library quantification and characterization were assessed with Agilent BioAnalyzer HS DNA Kit (#5067-4626) and the Invitrogen Qubit DNA HS Assay Kit (#Q32854). Libraries were pooled together with other index – compatible RNA-seq libraries for sequencing on Illumina NovaSeq 6000 (San Diego, CA) paired-end 100bp flow cell to a minimum depth of 20 million clusters per sample.

Upon data collection, the raw reads were first cleaned by removing adapter sequences and poly-x sequences (> 9 nt used for detection) using fastp (Version 0.20.0).[88] Sequence pseudo alignment of the resulting high-quality reads to the *Mus musculus* reference genome (build GRCm39) and quantification of gene level expression (gene model definition from GENCODE release M31) was carried out using Kallisto (Version 0.46.1).[79] To detect differentially expressed genes we used the glm approach implemented in the software package DESeq2 (R version: 4.2.2, DESeq2 version: 1.38.0).[89] Genes showing altered expression with adjusted p-value <= 0.05 and log2 ratio >= 0.5 were considered significant. Over-representation analysis (ORA) of gene ontology biological process (BP) terms was conducted based on differentially expressed genes with p-value < 0.01 using clusterProfiler (Version 4.6.0).[90] Terms with a false-discovery rate < 0.05 were considered significant.

Statistical analysis

GraphPad Prism 7 (GraphPad Software, San Diego, CA, USA) was used for statistical analysis. The sample sizes in each experiment are provided in figure legends. The data are presented as mean ± SEM. Statistical significance was defined as $P < 0.05$ and determined by two-tailed t-test or one- or two-way ANOVA, with Tukey and Bonferroni post-hoc analysis. For RNA sequencing analysis, statistical significance was determined as described in 'RNA sequencing analysis'.